Lawrence Berkeley National Laboratory
Recent Work

Title
THE INVESTIGATION OF HIGH STRENGTH IN HIGH CARBON STAINLESS STEEL

Permalink
https://escholarship.org/uc/item/0q47w76c

Author
Sauby, Michael E.

Publication Date
1970-09-01

UCRL-19678

c. 2

THE INVESTIGATION OF HIGH STRENGTH IN
HIGH CARBON STAINLESS STEEL

Michael E. Sauby
(M.S. Thesis)

Sept. 1970

LAWRENCE RADIATION LABORATORY
UNIVERSITY of CALIFORNIA BERKELEY

UCRL-19678

DISCLAIMER

CONTENTS

THE INVESTIGATION OF HIGH STRENGTH IN HIGH CARBON STAINLESS STEEL

Michael E. Sauby

Inorganic Materials Research Division, Lawrence Radiation Laboratory,
Departmart of Materials Science and Engineering, College of Engineering,
University of California, Berkeley, California

ABSTRACT

Factors necessary for the development of high strength with retention of ductility in austenitic stainless steels have been studied. Two thermo-mechanically worked alloys of the 18 Cr-8 Ni type containing carbon contents of 0.13 wt % and 0.33 wt % have been found to have yield strengths at least four times that observed in annealed Type 302 stainless steels. In the low-carbon alloy, elongations in excess of 40% are observed in the as-rolled samples. In the 0.33% C alloy the elongation increases from less than 10% to more than 40% during the course of an 8 hour aging period. Two higher carbon alloys, 0.46% and 0.56% C, showed slightly higher strength but much lower elongation.

Weight loss in a boiling nitric acid-dichromate solution demonstrates that the four alloys studied have much lower corrosion rates than annealed samples of Types 302 and 304 stainless steels. The observed difference in corrosion rates is due to the combination of higher purity and excellent dispersion of carbides. Weight loss through grain removal is an important mechanism in the 302 and 304 samples but not in the four alloys used in this investigation.

I. INTRODUCTION

In most cases where high strength is desired in an austenitic
stainless steel it must be obtained through cold rolling. With a 60%
reduction by cold rolling of a Type 302 stainless steel, yield strengths
of 180,000 psi and tensile strengths of 206,000 psi can be obtained.
But the elongation after this treatment is only about 3% (1).

It should be possible to use thermomechanical treatments to develop
comparable strengths with large elongations. This method of processing
has been shown to be of value in the development of TRIP (Transformation
Induced Plasticity) steels (2-4). The major factor in the improvement
of properties through the TRIP phenomenon are the proper alloy content to
induce a highly strain hardened austenite, a good dispersion of carbides,
and an austenite stability of the proper magnitude to undergo the $\gamma \rightarrow \alpha'$
transformation in areas demonstrating premature necking. Bressonelli and
Moskowitz (5) showed that early necking and failure could be prevented
by increasing the strain-hardening rate in localized regions through
strain induced transformation to martensite.

Little work has been done on the corrosion properties of a thermo-
mechanically worked stainless steel. One method of evaluating the inter-
granular corrosion resistance of a stainless steel is that used by
Aust, et al. (6). They showed that through the proper heat treatment
discrete globular carbides were formed in the grain boundaries, thereby
reducing intergranular attack. The creation of a similar structure
throughout the microstructure should produce generally greater corrosion
resistance.

II.   EXPERIMENTAL PROCEDURE

A.   Material Preparation

Table I lists the compositions of the alloys studied and of commericial Types 302 and 304 stainless steels. Alloy A (0.13% C) was prepared to be within the composition limits for a Type 302 stainless steel. Three of the alloys (B, 0.33% C; C, 0.46% C; and D, 0.56% C) were selected on the basis of the composition limits for pure austenite at 1150°C given by Bain and Paxton (7). It was desirable to have high chromium and carbon content for corrosion resistance and strength. Nickel was added to stabilize the austenite at room temperature.

The alloys were prepared as 16-pound ingots by induction melting in an argon atmosphere and pouring into copper molds. The resulting ingots were then homogenized at 1100°C for three days; the ingots were placed in steel tubes and surrounded by cast iron chips to reduce decarbonization. Upon completion of homogenization the ingots were ice-brine quenched. The scale was removed by sand-blasting and casting defects (voids and cracks) were ground out.

B.   Thermomechanical Treatments

Alloys A and B were upset forged at 1100°C to 5/8 in. X 2 in. The cracks formed during forging were removed by milling about 0.30 in. from each face. Further reduction was obtained by rolling at 1100°C to 0.250 in. After all surface cracks were ground out the samples were solution treated at 1300°C for 1 hour. An ice brine quench followed each one of the above higher temperature processing steps.

Alloys C and D were initially forged to 1 in. X 1-5/8 in., rolled at

1100°C to 0.500 in. and solution treated for 2 hours at 1250°C with an ice brine quench following each step. The samples were then rolled to 0.250 in. at 1100°C and ice brine quenched. Finally, the surface cracks were ground out and the samples were solution treated at 1300°C for one hour followed by an ice-brine quench. Alloys C and D were processed first and plans were initially made to try to achieve prior deformation to 90%. Preliminary tests indicated that deformation past 80% was impractical.

Alloys A and B were reduced to 0.050 in. by rolling at 500°C with heated rolls. Between passes the samples were reheated in an electric furnace held at 500°C. Alloys C and D were reduced to 0.066 in. by rolling at 500°C. Further deformation was limited by severe cracking.

Tensile specimens machined to the specifications of Fig. 1 were aged at 500°C for intervals of 1, 2, 4, 8 and 16 hours, with a 32-hour aging time added for alloy B. The as-rolled specimens are assumed to have received approximately 0.1 hour aging when reheated prior to the last pass through the rolls. Specimens of alloy B were aged also at 525°C for selected time intervals.

Three specimens each of alloys C and D were reduced in thickness by grinding to be used in permeability studies.

C. Mechanical Testing

Tensile tests were conducted at room temperature with an Instron Testing Machine. Alloy A was tested at a crosshead rate of 0.04 in./min and alloys B, C and D were tested at a crosshead rate of 0.02 in./min. A few specimens of alloy B were tested at a crosshead rate of 0.04 in./min to determine if there might be any strain-rate effect in this alloy.

D. Magnetic Testing

The saturation magnetizations of several specimens were determined quantitatively to measure the amount of magnetic phase present before and after tensile testing.

The fraction of magnetic phase was determined through the ratio B_s/B_o, where B_s is the saturated induction of the sample and B_o is the saturated induction of a completely martensitic specimen. B_o varies with alloy content and can be calculated theoretically (8). The experimental apparatus has been described previously (9).

E. X-Ray Diffraction

As-rolled samples of alloys A, B, C and D and a sample of B aged 8 hours at 500°C were mounted in bakelite, ground through 600 grit silica paper, and polished on a 0.5 μ diamond-paste-impregnated wheel. The samples were then examined on a Norelco diffractometer, equipped with a diffracted beam (200) - LiF crystal monochromator used with CuK_α radiation. The Bragg angle (2θ) was varied from 35° to 70° at a rate of 1°/min. A curve for bakelite was run to enable definite identification of those peaks belonging to the sample.

F. Optical and Electron Microscopy

Polished specimens of alloys A, B, C and D were etched with aqua regia (10 ml. HCl, 5 ml. HNO_3 and 5 ml. H_2O). A Carl Zeiss optical microscope was used for observation under incident and cross-polarized light.

Carbide extraction replicas were prepared for a series of samples of different aging times of alloy B. The samples were polished and deeply etched with aqua regia prior to replication. The replicas were removed

by electropolishing in a 10% perchloric acid, 90% acetic acid solution at about 20 volts.   The replicas were examined at 100 kV in an Hitachi HU-125 electron microscope.

G. Corrosion Tests

The corrosion resistance of alloys A, B, C and D were compared with samples of commercially available annealed sheets of Types 302 and 304 stainless steels. These tests are similar to those discussed by other authors (6, 10-14).

A boiling solution (109°C) of 5 N HNO_3 containing 11.3 gm/l of potassium dichromate was used in this study. The solution was contained in a spherical three-necked, 2000-ml flask. Two of the necks were plugged and a condensor was attached to the third. The solution was heated using a hemispherical heating mantle.

One-half inch disks machined from the sheet materials were used in this study. Prior to immersion the samples were ground through 600-grit silica paper, washed, and rinsed with distilled water. All seven specimens (A, as rolled; B, as rolled; B, aged 8 hours at 500°C; C, as rolled; D, as rolled; 302, and 304) were immersed simultaneously. The samples used showed enough variation in weight to be identified by weight differences.

For comparison purposes 1/4 in. X 1/4 in. X 1/2 in. samples of alloys A and B were cut from the 0.250 in. annealed bars prior to warm-working. These samples were prepared and tested in the same manner as the worked samples to more closely identify the benefits derived from the thermo mechanical treatments.

The samples were removed at approximately 2-hour intervals, rinsed, dried, and weighed on a Mettler analytical balance with an accuracy of

$\pm$ 0.1 mg.   The test solution was changed after 8 hours to reduce the

effects of a change in solution concentration.

III. EXPERIMENTAL RESULTS

A. Mechanical Testing

Tables II through VI list the mechanical properties of the alloys under consideration. Figures 2, 3, 5, 7 and 9 show the variations in tensile properties with aging of alloys A (aged at 500°C), B(500°C), B(525°C), C(500°C) and D(500°C).

Figure 2 summarizes the aging response of alloy A. Except for the slight reduction in tensile strength after 6 hours little response is observed in the yield or tensile strength. Both the reduction in area and elongation decrease slightly with aging time. The engineering stress-strain diagram for an as-rolled specimen of alloy A is shown in Fig. 3. The shape of the curve resembles those observed in TRIP steel, with long Luders strain followed by a serrated portion of positive strain-hardening rate.

As shown in Fig. 4, alloy B has a significant response to aging at 500°C. Figure 4a illustrates the precipitation hardening effect present in alloy B. The elongation as shown in Fig. 4b increases rapidly with aging at 500°C between 4 and 8 hours. There is a small increase in reduction in area corresponding to this increase in elongation.

The improvement in mechanical properties is indicated by the changes in the engineering stress-strain curve with aging as shown in Fig. 5. The curve for the as-rolled specimen shows instability as it necked and failed early in the test. The specimen aged for 8 hours at 500°C showed good stability. This curve is not as serrated as those observed in Alloy A and most TRIP steels.

Tensile tests with specimens of alloy B failed to show that there were any differences in mechanical properties between strain rates of 0.02 and 0.04 in./min.

Figure 6 shows changes in mechanical properties with aging at 525°C. After aging at 525°C alloy B shows slightly different properties than when aged at 500°C. The yield strength at 525°C shows a slight peak similar to that observed at 500°C, but the tensile strength decreases with aging time. But the major difference between the two aging temperatures is seen in the response of the elongation to aging. At 500°C there is an apparent increase in elongation of about 37% while at 525°C the increase is only about 29%. This difference may be due to incorrectly fixing the peak in Fig. 6. The actual peak at 525°C may be between 2 and 4 hours rather than as indicated.

Slight peaks in the yield and tensile strength are possibly observed in alloy C after about 1 hour at 500°C as shown in Fig. 7a. The reduction in area is seen to decrease with aging time except for the region between 1 and 5 hours where the reduction in area is observed to be approximately constant. Little change is observed in the elongation, as shown in Fig. 7b. The shape of the engineering stress-strain curve for an as-rolled specimen of alloy C is shown in Fig. 8a.

Small peaks in the yield and tensile strengths were observed in alloy D with aging as shown in Fig. 9a. The reduction in area is observed to decrease steadily with aging while the elongation remains fairly con-stant. An engineering stress-strain diagram for alloy D is illustrated in Fig. 8b.

The relationship between carbon content and yield strength for 80% deformation is shown in Fig. 10. The point at 0.02% C was extrapolated

from the data of Floreen and Tufnell (15). There appears to be a slightly parabolic function for the dependence of the yield strength upon carbon content. Since alloys C and D were only deformed about 73%, the curve has been drawn slightly above the points for these alloys to represent more closely the effect of carbon in an alloy receiving 80% prior deformation.

B. Magnetic Testing

The amount of magnetic phase present was found to be very low in specimens whose saturation induction was determined prior to mechanical testing. The amount of magnetic phase present in the as-rolled specimens appear to be independent of carbon content: 0.3% in alloy A, 0.2% in B, 0% in C, and 0.4% in D. After 8 hours at 500°C the fraction of magnetic phase in alloy B has risen to about 0.6%.

In the specimens of alloys A (as rolled) and B (aged 8 hours, 500°C) showing good elongations, a large amount of magnetic phase was observed. A specimen of alloy A having an elongation of about 41% showed an increase in the fraction of magnetic phase to 74%. A specimen of alloy B aged 8 hours at 500°C showed only about 39% magnetic phase after mechanical testing.

In alloys C and D little increase in martensite was observed; i.e., about 0.6% and 0.5%, respectively, after mechanical testing. In both cases the fracture was not in the center of the gage length, therefore, the actual amount of transformation may be larger. With a hand-held magnet the necked region of both specimens is highly magnetic.

C. X-Ray Diffraction

The diffractometer curves obtained from samples of alloys A (as rolled), B (as rolled), B (aged 8 hours, 500°C), C (as rolled), and D (as rolled) indicated that no phases were present except austenite.

The $(200)_\gamma$ peak was observed only in alloy A. This peak rose about 20 counts per second (cps) above the noise while the $(111)_\gamma$ peak rose about 400 cps above the noise.

The $(111)_\gamma$ peak rose to an intensity of about 404 cps in the as rolled sample of alloy B. In the sample of B aged 8 hours at 500°C to $(111)_\gamma$ peak showed a further decrease in intensity in alloys C and D; 144 cps and 104 cps, respectively.

D. Optical and Electron Microscopy

Some of the results of metallographic studies are presented in Figs. 11 through 18. In Fig. 11a the banding present in alloy A can be seen as well as the good dispersion of precipitates created by warm rolling (500°C).

Figure 11a also shows that precipitation has occurred along slip bands and that very little precipitation has occurred in the grain boundaries. Figure 11b shows more clearly that the precipitates have formed along slip bands in the austenite.

Banding is also observed in the as-rolled sample of alloy B, but the precipitation is heavy and fairly uniform throughout most of the structure as shown in Fig. 12a. The irregular structure of alloy B is shown in Fig. 12b at higher magnification.

Figure 13 is an electron micrograph showing the small size of the precipitates in the austenite of the as-rolled samples of alloy B. These needle shaped precipitates have been identified as Cr_7C_3 from electron diffraction patterns.

The severe delamination and longitudinal cracking that occurred in a specimen of alloy B aged 8 hours at 500°C is shown in Fig. 14. This indicates that the mechanical properties can be expected to be very anisotropic in this type of material. Between areas of delamination the failure appears to have been by a shear mode. Figure 15 shows the heavy precipitation in this aged sample.

Upon overaging, fine precipitates of $Cr_{23}C_6$ have formed in the grain boundaries as shown in Fig. 16 of a specimen aged for 16 hours at 500°C. The precipitates are about 600 Å in size. In the as-rolled condition there were no areas observed that contained $Cr_{23}C_6$ precipitates. Diffraction patterns from the area shown in Fig. 16 indicate that two types of precipitates are present, $Cr_{23}C_6$ in the grain boundaries and both Cr_7C_3 and $Cr_{23}C_6$ in the austenite.

Figure 17a shows some of the banding present in an as-rolled specimen of alloy C. The microstructure is also observed to have a high volume fraction of small precipitates with some large precipitates throughout the structure. In Fig. 17b the majority of the precipitates are observed to be very small and well dispersed and the precipitation along the grain boundary is discontinuous.

Figures 18a and 18b show the precipitation along slip lines and in slip bands of alloy D. Figure 18a shows that the majority of the precipitates had formed in the deformed austenite rather than at the grain boundaries.

E. Corrosion Resistance

The susceptibility to attack of the Types 302 and 304 stainless

steels and the four thermomechanically worked alloys in a solution of

5N HNO_3 containing 11.3 gm/l of potassium dichromate are summarized in

Figs. 19 and 20.

Figure 19a illustrates the behavior of the Type 302 annealed sheet

used in this study and the various heat-treated samples of 302 used by

Aust, et al. (11). The curves exhibit steady state corrosion rates of

(a) 4.8 mg/cm^2/hr; (b) 8.3 mg/cm^2/hr; (c) 3.1 mg/cm^2/hr; and

(d) 9.3 mg/cm^2/hr. Optical examination of the surface showed severe

general attack.

Figure 19b shows the behavior of the Type 304 sample used in this

study and the variously heat-treated samples used by Aust, et al. (11).

The steady state corrosion rates are (a) 4.2 mg/cm^2/hr; (b) 6.2 mg/cm^2/hr;

and (c) 1.9 mg/cm^2.hr.

The corrosion behaviors of alloys A, B, C and D are summarized in

Fig. 20. The five curves of Fig. 20 show that there is no incubation

period in a thermomechanically worked stainless steel. The samples of

Types 302 and 304 stainless steel used in this study show a corrosion

rate more than an order of magnitude greater than that for any of the

alloys prepared for this study.   The corrosion rates of the various

samples are listed in Table VII. The differences in the surface attack

can be seen in Fig. 21. The samples of 302 and 304 are observed to be

deeply and evenly attacked while alloys A, B (as rolled and aged 8 hours

at 500°C), C and D are observed to be lightly etched.

The comparison tests run with undeformed samples of alloys A and

B show that there is no appreciable difference in the corrosion rate

between samples annealed at 1300°C and similar samples that have been reduced 80% by rolling at 500°C. In alloy A the deformation appears to have aided the corrosion resistance by reducing the rate from 0.24 mg/cm^2/hr in the annealed sample to 0.21 mg/cm^2/hr in the deformed sample. But in alloy B a slight increase in corrosion rate from 0.19 mg/cm^2/hr to 0.20 mg/cm^2/hr is observed after deformation.

IV. DISCUSSION

A. Mechanical Properties

The development of high yield strengths in austenitic steels can be attributed to two main phenomena:

(1) the increase in the strength of the austenite through strain hardening during thermomechanical working, and

(2) development of a fine dispersion of carbides during the thermomechanical treatment.

In a very low carbon austenitic stainless steel (12 Ni-18 Cr-0.02 C) receiving prior deformation at 525°F an increase in yield strength was found with increasing deformation (15). The majority of the increase in strength is due to the strain hardening of the austenite since the volume fraction of precipitates formed would be very small in this alloy. With increasing carbon content the increase in strength can be associated with the formation of alloy carbides. This is partly due to dispersion strengthening, but the carbides also affect the rate of strain hardening of the austenite at elevated temperature so as to produce a more highly dislocated structure. Figure 10 shows that a significant increase in strength is obtained with carbon. The rate of increase appears to decline after about 0.5%C.

Several authors have discussed the importance of carbide formers in ausforming (2,3, 16-18). They have found that a high dislocation density is important to the creation of a fine dispersion of carbides. An increased dislocation density provides not only more nucleation sites for carbides to form but also aids vacancy enhanced diffusion of substitutional atoms. An important consideration in thermomechanical working must be

the temperature of deformation. McEvily, et al. (16) and Kula (19) have stressed the importance of a deformation temperature corresponding to that at which alloy carbides form, but not so high as to cause re-crystallization.

Figure 13 show precipitates of Cr_7C_3 formed during the deformation of alloy B at 500°C. These precipitates are finely spaced, i.e. about 0.35μ.

Examination of the microstructure has indicated that precipitation is fairly uniform throughout the matrix. Figure 11 shows clearly that precipitation has occurred along deformation bands in alloy A. This type of precipitation can lead to the fine dispersions observed.

Of the four alloys tested, alloys A and B demonstrated the most interesting results. Both had high strengths and demonstrated a signifi-cant amount of ductility after proper heat treatment. Alloys C and D both showed high strength but did not demonstrate large elongations.

High strengths and ductilities have been observed in a number of austenitic steels (2-4). The high ductilities observed have been found to be due to strain induced transformations of austenite to martensite. The high values of ductility are observed when the austenite is just unstable enough to prevent necking by the $\gamma \rightarrow \alpha'$ transformation, but not so unstable as to cause rapid work-hardening.

Bressanelli and Moskowitz (5) showed that, by increasing the rate of strain hardening through transformation, failure by early necking could be prevented. In highly stable austenite the work hardening rate is not sufficient to provide the needed strengthening during necking. But in a metastable austenitic steel the transformation to martensite

can occur in the areas of highest strain thereby increasing the strength. Therefore, localized flow is reduced and uniform strain along the gage length is promoted.

The stability of the austenite in an alloy can be calculated using the empirical results of Angle (8). He defines stability in terms of $M_{d_{30}}$. As used here, $M_{d_{30}}$ will be the temperature suggested by Angle (8) at which 50% martensite is formed in tension after a true strain of 0.30. The $M_{d_{30}}$ temperature can be characterized by

$$M_{d_{30}} (°C) = 413-462[C+N]-9.2[Si]$$
$$- 8.1[Mn]-13.7[Cr]-9.5[Ni]$$
$$- 18.5[Mo],$$

where [x] equals the weight percent of the individual alloying elements.

The $M_{d_{30}}$ temperature of alloy A was calculated to be 30°C. In room temperature tests, this alloy would be expected to undergo some strain-induced transformation. This was found to be the case, with alloy A showing excellent elongations.

The stress-strain curve of alloy A shown in Fig. 3 is similar to that observed for some TRIP steels (2-4), i.e., high yield strength and long Luders strain followed by an increase in the strain hardening rate with the final portion of the curve serrated. The trend in the tensile data indicating a decrease in elongation with aging time (Fig. 2a) can be attributed to further reduction in the stability of the austenite as carbides are precipitated.

The measurement of saturation magnetization demonstrates that strain induced transformation is an important factor in the elongation (3,9). In the case of alloy A, an as-rolled specimen showed a volume

fraction of magnetic phase of less than 0.3%. After testing, the amount of martensite detected was 74%. This large amount of transformation, especially at points of necking, is responsible for the good elongations.

Of special interest in this investigation is the response of alloy B to aging. With a calculated $M_{d_{30}}$ of $-30°C$, this alloy had fair ductility in the as-rolled condition (about 9% elongation).

Upon aging, a definite increase in ductility is observed. In the course of the first 8 hours of aging the elongation has increased from about 9% to 45%. During this aging period additional carbides were precipitated causing small increases in strength. This precipitation also acts to reduce the effective alloy content of the austenite decreasing its stability. McEvily et al. (16) have noticed that precipitation can lead to reduced amounts of carbon in the area surrounding the austenite, leading to local elevation of $M_{d_{30}}$. In the case under consideration the volume fraction of precipitates is large and the dispersion is fine. Therefore, increased precipitation will lead to general elevation of the $M_{d_{30}}$ temperature.

In studying carbide extraction replicas it is found that a transition is occurring in the type of precipitates observed with increasing aging time. The volume fraction of Cr_7C_3 is decreasing and a fine dispersion of $Cr_{23}C_6$ is being formed. The transition from Cr_7C_3 to $Cr_{23}C_6$ may explain some of the increase in strength.

The change in the stress-strain curve of alloy B as a result of aging is shown in Fig. 5. After aging 8 hours at $500°C$ the transformation was not sufficient to cause an increase in the strain hardening rate but the strain hardening rate was sufficiently increased to prevent

necking and result in a larger Luders strain and total elongation. In

alloys A and B the austenite lacks the strain-hardening capacity to

overcome necking and transformation to martensite is necessary to produce

uniform elongations.

To produce approximately the same elongations in alloys A and B,

51% and 47% respectively, strain induced transformations of about 75% and

39% respectively were needed. The austenite in the higher carbon alloy,

therefore, has a high enough strain hardening rate to overcome a greater

proportion of the necking instability without transformation.

The austenite stability of alloys C and D, $M_{d_{30}}$ ' temperatures of

-138°C and -135°C, respectively, is found to be too high to enable good

elongation to be obtained.

The results of the X-ray diffraction study indicate that no major

phases other than carbides are present in the austenite that might affect

the mechanical properties. Therefore, the observed properties are merely

a function of the austenite strength and stability.   There are con-

flicting theories as to the effect of prior deformation upon the micro-

structure. Mangonon and Thomas (20) observed that ε-martensite (a para-

magnetic phase) is formed during rolling at liquid nitrogen temperature.

But Floreen and Mihalisin (21) have raised doubts that ε is formed by

rolling. The diffraction curves obtained in the present study seem to

indicate that no ε martensite is formed during rolling at 500°C. This

might be expected since Mangonon and Thomas (20) found that 200°C was

near the temperature at which ε-martensite begins to revert to austenite.

But, it is possible that the rolling texture of these samples plus the

presence of carbides would mask the presence of small amounts of additional

phases. The volume fraction of precipitates appears to affect the dif-
fractometer curve as noted in Section III-C. The decrease in the intensity
of the $(111)_\gamma$ peaks in the aged sample of alloy B and the as-rolled
samples of alloys C and D indicates that the austenite is strained by in-
creasing numbers of carbides causing microabsorption, thereby reducing the
intensity.

B.   Corrosion Resistance

In addition to the development of improved mechanical properties
very desirable corrosion resistance is found to be present after thermo-
mechanical treatments. The results of the present investigation indicate
that the thermomechanically worked steels studied have much greater cor-
rosion resistance in a boiling nitric acid-dichromate solution than the
annealed commercial samples of Types 302 and 304 stainless steels.

It is possible that the improvements in corrosion resistance are not
entirely due to the thermomechanical treatments. For example, Armijo (14)
has shown that corrosion resistance in the nitric acid-dichromate test
solution can be strongly influenced by the impurity elements phosphorus
and silicon. Excessive additions of phosphorous ($> 10^2$ ppm) and silicon
(between 2×10^3 ppm and 2×10^4 ppm) can seriously detract from the cor-
rosion resistance.

The work of Armijo (14) on the effect of phosphorus on the corrosion
rate would tend to indicate that the 302 and 304 samples tested would have
a corrosion rate four times as fast as that observed in alloys A, B, C
and D if other variables were equal. Therefore, an important factor in
the improvement in properties may be the lower phosphorus content of
the worked alloys.

The large differences in corrosion rates with variations in silicon content determined by Armijo (14) in a high purity 14 Cr-14 Ni-Fe alloy may only be partly applicable to nominal 18 Cr-8 Ni-Fe alloy. If the variation in rate of attack with silicon content held true, the 302 sample used in this investigation would have a corrosion rate about five times as fast as the 304 sample used. However, it was found that the difference was negligible. Therefore, the effect of silicon in this type alloy (nominal 18 Cr-8 Ni) may be subject to question. In a quenched alloy very little effect is found with carbon content (14), therefore, this is not considered a major factor in the current study.

The samples of 302 and 304 stainless steels used in this investigation for comparison purposes show some discrepancies from results of Aust, et al. (11). Within Figs. 19a and 19b, curves (a) and (b) are for similarly heat-treated materials. The discrepancies may be due to differences in annealing temperature and time. No control was exerted over the commercial alloys used in this study. Small differences in alloy composition (14) and concentration differences in the nitric acid-dichromate solution (10) may lead to variations in the results.

Significant improvements in corrosion resistance of annealed 302 and 304 stainless steels have been realized through selected heat treatments (11). A two hour heat treatment at 850°C followed by a water quench was shown to decrease the corrosion rate of a 302 annealed sample from 8.3 mg/cm^2/hr (curve (b) Fig. 19a) to 3.1 mg/cm^2/hr (curve (c)) (11). A similar heat treatment in a 304 sample at 900°C reduced the corrosion rate from 6.2 mg/cm^2/hr (curve (b) Fig. 19b) to 1.9 mg/cm^2/hr (curve (c)).

It is believed that the carbides formed during the heat treatment incorporate solute impurities from the grain boundary region (6). The

highest rates of corrosion were observed in the annealed samples having

no carbides in the grain boundaries and in samples having a continuous

carbide phase in the grain boundaries. The lowest corrosion rates were

found to correspond to the presence of isolated carbides at grain bound-

aries (6, 11). The model of solute segregation at grain boundaries is

further confirmed by the observation of Armijo (12) that the corrosion

rate can be reduced by high temperature solution treatment. At solution

temperatures approaching the melting temperature susceptability to cor-

rosion is reduced through desorption of impurities.

From the observations made by previous investigators (6, 11, 14) it

may be possible to explain the excellent corrosion resistance of alloys

A, B, C and D, in a boiling nitric acid-dichromate solution. The purity

of the alloys, especially the low phosphorus content, must be an im-

portant factor in the low corrosion rates. But, a significant part of

the corrosion resistance must be due to the heat treatments that these

four alloys received.

The low corrosion rates in the annealed samples of alloys A and B

must be due to the alloy purity and the high anneal temperature used.

After annealing at 1300°C the solute impurities are more evenly dis-

tributed throughout the microstructure rather than at the grain bound-

aries.

After thermomechanical working the excellent corrosion resistance

is believed to be due to a combination of the alloy purity and the dis-

persion of carbides produced at the rolling temperature. As observed

in the micrographs the dispersion of carbides is fine, with no continuous

carbide paths observed even in the higher carbon alloys. The dispersion

of carbides is such that nearly all of the harmful impurities should be absorbed.

It is difficult to visualize the electrochemical process that must be responsible for the excellent corrosion resistance in the thermo-mechanically worked samples of alloys A, B, C and D. No incubation period is observed in alloys A, B, C or D as opposed to 302 and 304. This would indicate uniform attack. Another factor which must be considered also is the austenite grain size. The small grain size in the 302 and 304 samples would enable weight loss to occur through removal of entire grains while in alloys A, B, C and D the grain size is so large that weight loss can occur only by chemical attack and not by grain removal.

But it would be expected that in a highly deformed alloy the free energy would be so high that electrochemical attack should be enhanced. Residual stresses around particles may cause an increase in chemical attack (22). It is also possible that plastic deformation at the tips of the grain boundary grooves may lead to an increase in the intergranular penetration rate (10). The fine dispersion of precipitates should lead to many small electrochemical cells in the austenite leading to higher cor-rosion rates. The high irregularity produced in the grain boundaries through the large deformation in processing should also contribute to an increase in the corrosion rate.

The means by which thermomechanical working can reduce the chemical attack in a nitric acid-dichromate solution is not clear. If the impurity solute segregation is the primary factor in raising the corrosion rate then the fine dispersion of precipitates would absorb the impurities very effectively throughout the microstructure. It may be possible that each

precipitate forms an electrochemical cell with the austenite and that these very small cells may interact in some manner so as to reduce the overall effect.

V. CONCLUSIONS

This investigation was undertaken to determine the possibility of developing a high strength austenitic stainless steel through alloy control and thermomechanical treatments.

It has been shown that a stable austenitic stainless steel similar to a Type 302 can be made to show a two fold increase in tensile strength and a four fold increase in the yield strength through thermomechanical treatments. The increased strength of the alloys is obtained with no significant loss in ductility. The strain-induced transformation observed during testing is an important factor in the retention of ductility.

Through the addition of carbon an austenitic alloy of higher stability has been obtained. Alloy B (0.33% C) was found to possess yield and tensile strengths in excess of 200,000 psi. The stability of the austenite detracted from the elongation observed in the as-rolled samples. But upon aging, the precipitation of carbides has reduced the effective alloy content of the austenite enough so that strain induced transformation can contribute to the deformation, leading to excellent elongation.

In comparison tests with samples of 302 and 304 stainless steels, the alloys developed for this investigation were found to be far superior in corrosion resistance. The differences in corrosion rates are due to a combination of differences in purity and the fine dispersion of precipitates created during the thermomechanical treatments. It has been suggested that by reducing solute impurities through absorption into the carbides the corrosion resistance can be improved. But some other undetermined factor is probably more important in this reduction in corrosion rate. The austenite grain size effect may also have an important role in the

low rates observed.   In alloys A, B, C, and D the grain size is so
large that weight loss will only occur by chemical attack for a long
period of time rather than through grain removal as observed in the much
finer grained 302 and 304 stainless steels.

VI.   SUGGESTIONS FOR FUTURE STUDY

1. Investigate the effect of thermomechanical treatments on the mechanical and chemical properties of a commercial purity stainless steel.

2. A comparison test of annealed and thermomechanically worked commercial stainless steel to determine the effect of warm working on corrosion resistance of samples of approximately equal grain size. A small grain size would be desirable to determine if weight loss through grain removal can be deterred.

3. Potentiodynamic corrosion tests should be run to determine if the corrosion resistance of the present alloys are as good relative to 302 and 304 samples in a different electrochemical system.

ACKNOWLEDGMENTS

REFERENCES

1. <u>Mechanical and Physical Properties of Austenitic Chromium-Nickel Stainless Steels at Ambient Temperatures</u> (International Nickel Co., New York, 1963).

2. V. F. Zackay, E. R. Parker, D. Fahr, and Raymond Bush, The Enhancement of Ductility in High-Strength Steels, Trans-ASM, <u>60</u>, 252 (1967).

3. J. A. Hall, V. F. Zackay and E. R. Parker, Structural Observations in a Metastable Austenitic Steel, Trans-ASM (to be published).

4. D. Fahr, Enhancement of Ductility in High Strength Steels, (Ph. D. thesis) University of California, Berkeley, UCRL-19060, Sept. 1969.

5. J. P. Bressanelli and A. Moskowitz, Effects of Strain Rate, Temperature, and Composition on Tensile Properties of Metastable Austenitic Stainless Steel, Trans-ASM, <u>59</u>, 223 (1966).

6. K. T. Aust, J. S. Armigo and J. H. Westbrook, Heat Treatment and Corrosion Resistance of Austenitic Type 304 Stainless Steel, Trans-ASM, <u>59</u>, 544 (1966).

7. E. G. Bain and H. W. Paxton, <u>Alloying Elements in Steel</u> (American Society for Metals, Metals Park, 1966).

8. T. Angle, Formation of Martensite in Austenitic Stainless Steels, J. Iron Steel Inst., <u>177</u>, 165 (1954).

9. B. de Miramon, Quantitative Investigation of Strain Induced Strengthening in Steel (M. S. thesis) University of California, Berkeley UCRL-17849, 1967.

10. J. S. Armijo, Intergranular Corrosion of Nonsensitized Austenitic Stainless Steels - I. Environmental Variables, Corrosion, <u>21</u>, 235 (1965).

11. K. T. Aust, J. S. Armijo, E. F. Koch and J. H. Westbrook, Inter-granular Corrosion and Electron Microscopic Studies of Austenitic Stainless Steels, Trans. ASM, $\underline{60}$, 360 (1967).

12. J. S. Armijo, Impurity Adsorption and Intergranular Corrosion of Austenitic Stainless Steel in Boiling $HNO_3-K_2Cr_2O_7$ Solutions, Corrosion Science, $\underline{7}$, 143 (1967).

13. K. T. Aust, J. S. Armijo, E. F. Koch, and J. H. Westbrook, Inter-granular Corrosion and Mechanical Properties of Austenitic Stain-less Steels, Trans. ASM, $\underline{61}$, 270 (1968).

14. J. S. Armijo, Intergranular Corrosion of Nonsensitized Austenitic Stainless Steel, Corrosion, $\underline{24}$, 24 (1968).

15. S. Floreen and G. W. Tuffnell, A Comparison of Ausforming to Cold Rolling for Strengthening Stainless Steel, T rans. ASM, $\underline{57}$, 301 (1964).

16. A. J. McEvily, Jr., R. H. Bush, F. W. Schaller, and D. J. Schmatz, On the Formation of Alloy Carbides During Ausforming, Trans-ASM, $\underline{56}$, 753 (1963).

17. L. Raymond, W. W. Gerberich and C. F. Martin, Strain Hardening of Austenite and its Effect on Subsequently Transformed Martensite, J. Iron Steel Inst., $\underline{203}$, 933 (1965).

18. G. Thomas, N. Schmatz, and W. W. Gerberich, Structure and Strength of Some Ausformed Steels, High Strength Materials, V. F. Zackay, Ed. (John Wiley and Sons, Inc., New York, 1965) p. 251.

19. E. B. Kula, Strengthening of Steel by Thermomechanical Treatments, in Strengthening Mechanisms, Proceedings of the 12th Sagamore Army Materials Research Conference (Syracuse University Press, 1966) p. 83.

20. P. L. Mangonon, Jr. and G. Thomas, Structure and Properties of
     Thermal-Mechanically Treated 304 Stainless Steel, Met Trans., 1,
     1587 (1970).

21. S. Floreen and J. R. Mihalisin, High-Strength Stainless Steel by
     Deformation at Low Temperature, in Advances in the Technology of
     Stainless Steel and Related Alloys, ASTM Special Technical Publica-
     tion No. 369 (1965) p. 17.

22. A. B. Kinzel, Chromium Carbide in Stainless Steel, Trans. AIME,
     194, 469 (1952).

Table I. Chemical composition of alloys in weight percent

Ingot No.	Alloy	% Cr	% Ni	%C	%Mn	%Mo	%P	%Si	%S
					Weight Percent				
6911-18	A	17.84	7.81	0.13	0.02*	0.02*	0.004	0.04	0.007
6911-19	B	15.91	7.86	0.33	0.02*	0.02*	0.003	0.02	0.007
6911-20	C	19.29	7.59	0.46	0.05	0.02*	0.003	0.06	0.008
6911-21	D	15.59	7.80	0.56	0.06	0.02*	0.003	0.09	0.008
	302	17.85	8.31	0.06	1.71	---	0.025	0.42	0.025
	304	18.02	9.08	0.08	1.70	0.15	0.025	0.62	0.011

*Indicates "less than"

Table II. Mechanical properties of Alloy A

Aging Temp. °C	Aging Time hours	Y.S. 1000 psi	U.T.S. 1000 psi	% Elong. 1 inch	% Reduction in area
500	0.1*	153	185	51	54
500	0.1	156	180	41	52
500	0.1	157	182	35	53
500	1	161	183	37	53
500	1	160	181	39	49
500	2	158	179	37	42
500	2	159	179	39	56
500	4	160	183	41	53
500	4	151	184	44	52
500	8	164	181	39	47
500	8	145	181	39	54
500	16	156	179	37	54
500	16	154	181	36	48

*For this presentation as-rolled specimens are assumed to have been aged approximately 0.1 hours. This time represents the length of time that the samples were in the furnace before the last pass. The last pass contributes only approximately 1% to the total deformation.

Table III.   Mechanical properties of Alloy B

Aging Temp. °C	Aging Time hours	Y.S. 1000 psi	U.T.S. 1000 psi	% Elong. 1 inch	% Reduction in area
500	0.1	208	223	7	50
	0.1	208	223	8	58
	0.1	212	223	9	58
500	1	207	222	10	42
	1	212	222	11	49
500	2	210	224	11	54
	2	208	212	11	52
500	4	213	225	16	54
	4	213	221	22	55
500	8	212	223	43	54
	8	212	216	25	54
	8	217	226	47	49
500	16	221	226	40	39
	16	215	221	8	35
	16	206	213	47	51
500	32	205	215	26	29
	32	203	210	26	22
525	1	215	225	10	58
	1	209	219	9	55
525	2	199	214	15	37
	2	213	221	27	60
525	4	214	219	35	50
	4	213	218	42	33
525	8	200	220	12	24
	8	192	207	27	31
525	17	187	206	24	20

Table IV.   Mechanical properties of Alloy C

Aging Temp. °C	Aging Time hours	Y.S. 1000 psi	U.T.S. 1000 psi	% Elong. 1 inch	% Reduction in area
500	0.1	231	245	4	44
	0.1	226	240	5	44
	0.1	232	240	4	48
500	1	235	250	4	36
	1	230	242	6	40
500	2	231	246	6	45
	2	233	241	3	34
500	4	235	250	5	42
	4	229	245	6	42
500	8	232	244	4	43
	8	234	244	4	35
500	16	240	253	4	31
	16	226	241	4	29

Table V. Mechanical properties of Alloy D

Aging Temp. °C	Aging Time hours	Y.S. 1000 psi	U.T.S. 1000 psi	% Elong. 1 inch	% Reduction in area
500	0.1	240	247	3	44
	0.1	233	243	5	39
	0.1	230	242	5	43
500	1	242	246	4	35
	1	231	243	6	40
500	2	237	254	4	35
	2	237	247	6	37
500	4	239	251	4	33
	4	234	244	4	33
500	8	240	254	4	32
	8	237	247	5	40
500	16	240	246	3	31
	16	224	243	4	30

Table VI. Mechanical properties of commercial
Type 302 and Type 304 stainless steels

Alloy	Y.S. 1000 psi	U.T.S. 1000 psi	% Elong. 2 inches	% Reduction in area
302[a]	37[b]	90	55	65
304[a]	35[b]	85	55	65

a. Values taken from Metals Handbook, Vol. 1, 8th Edition, 1961.

b. 0.2% Offset yield strength

Table VII. Summary of corrosion resistance

Alloy	Corrosion rate ($mg/cm^2/hr$)
302	4.8
304	4.2
A	0.21
B (as rolled)	0.20
B (aged 8 hr, 500°C)	0.19
C	0.31
D	0.30
A (annealed)	0.24
B (annealed)	0.19

Figure Captions

Fig. 1. Diagram of tensile specimen.

Fig. 2. Effect of aging at 500°C on the mechanical properties of Alloy A.

Fig. 3. Engineering stress-strain curve for Alloy A as rolled.

Fig. 4. Effect of aging at 500°C on the mechanical properties of Alloy B.

Fig. 5. Engineering stress-strain curve for Alloy B showing the differences between the stress-strain curve of minimum elongation (as rolled) and the curve of maximum elongation. (aged 8 hours at 500°C)

Fig. 6. Effect of aging at 525°C on the mechanical properties of Alloy B.

Fig. 7. Effect of aging at 500°C on the mechanical properties of Alloy C.

Fig. 8a. Engineering stress-strain curve for Alloy C., as rolled.

Fig. 8b. Engineering stress-strain curve for Alloy D.,as rolled.

Fig. 9. Effect of aging at 500°C on the mechanical properties of Alloy D.

Fig. 10. Effect of carbon content on the yield strength of thermo-mechanically worked stainless steels (as rolled).

Fig. 11. Optical micrographs of Alloy A showing banding and preferential precipitation along slip bands during thermomechanical working at 500°C to 80% reduction in thickness.

Fig. 12a. Cross-section of Alloy B after 80% reduction at 500°C. Large volume fractions of precipitates are observed. (Taken with cross-polarized light).

Fig. 12b. Cross section of Alloy B illustrating discontinuous nature of grain-boundary precipitation and irregular structure.

Fig. 13. Electron micrograph of carbide extraction replica showing the needle shaped precipitates of Cr_7C_3 in the as rolled condition of Alloy B.

Fig. 14. Cross-section through fracture of Alloy B (aged 8 hours, 500°C) showing severe longitudinal cracking and delamination.

Fig. 15. Fine dispersion of precipitates in Alloy B after aging 8 hours at 500°C. (taken with cross-polarized lighting).

Fig. 16. Electron micrograph of carbide extraction replica from a sample of Alloy B aged 16 hours at 500°C. Fine particles of $Cr_{23}C_6$ are observed in the grain boundaries.

Fig. 17a. Cross-section of Alloy C showing banding and heavy precipitation.

Fig. 17b. Cross section of Alloy C showing heavy precipitation throughout structure and relatively discontinuous nature of precipitation in the grain boundary.

Fig. 18a. Cross-section Alloy D showing decorated slip lines.

Fig. 18b. Cross-section of Alloy D showing heavily decorated slip bands.

Fig. 19a. Corrosion of Type 302 stainless steel.

    (a) Commercial cold rolled and annealed sheet used in this study

    (b) 2 hours at 1050°C, and quenched

    (c) same as (a) plus 2 hours at 850°C, quenched

    (d) same as (a) plus 2 hours at 650°C, quenched (sensitized)

    (b, c, and d are from Aust, et al. Trans ASM, 60, 360 (1967).)

Fig. 19b. Corrosion of Type 304 stainless steel

    (a) Commercial cold rolled and annealed sheet used in this study.

    (b) 2 hours at 1050°C, quenched

    (c) 2 hours at 1050°C and cooled to 900°C within 20 min, held 2 hours at 900°C, quenched

    (b and c are from Aust, et al. Trans ASM, 60 360 (1967).)

Fig. 20. Corrosion of thermomechanically treated alloys.

    A. Alloy A

    B. Alloy B: as rolled and aged 8 hours, 500°C

    C. Alloy C

    D. Alloy D

Fig. 21. Surfaces of corrosion samples after 19 hours in boiling solution of 5N HNO_3 · containing 11.3 gm/l of potassium dichromate.
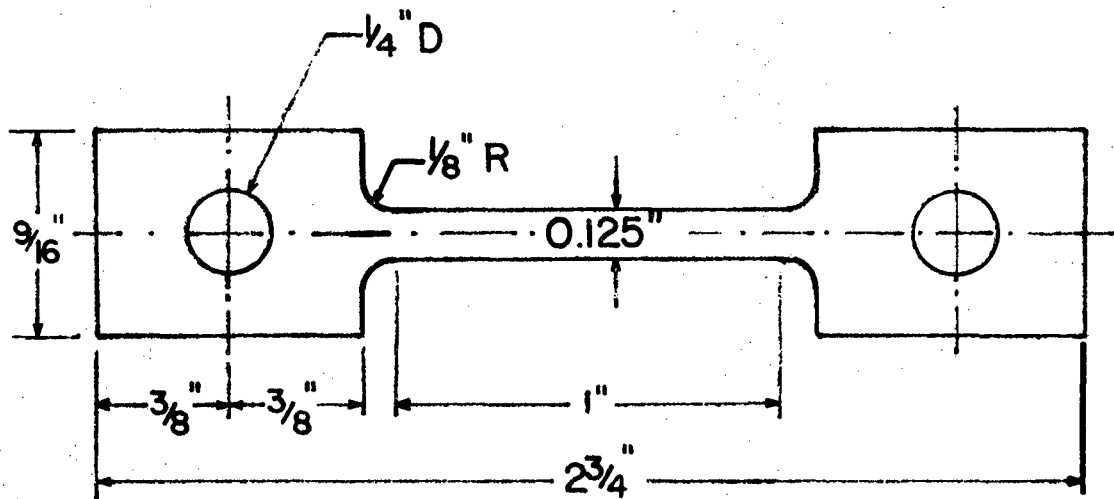
TENSILE SPECIMEN

SCALE: 2:1

XBL 698-1155

Fig. 1

XBL 708-1882

Fig. 2

ENGINEERING STRESS, 1000 PSI

ENGINEERING STRAIN, %
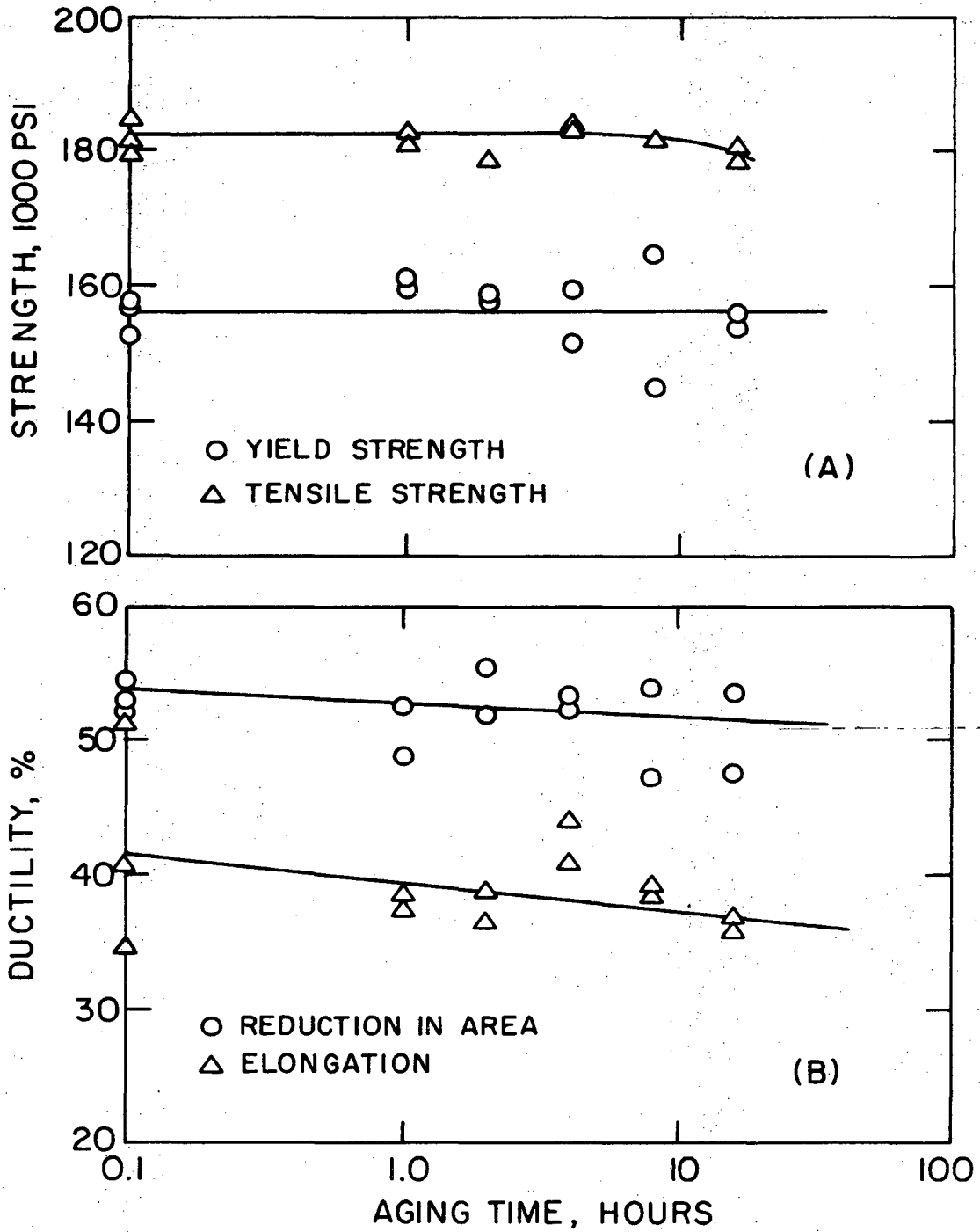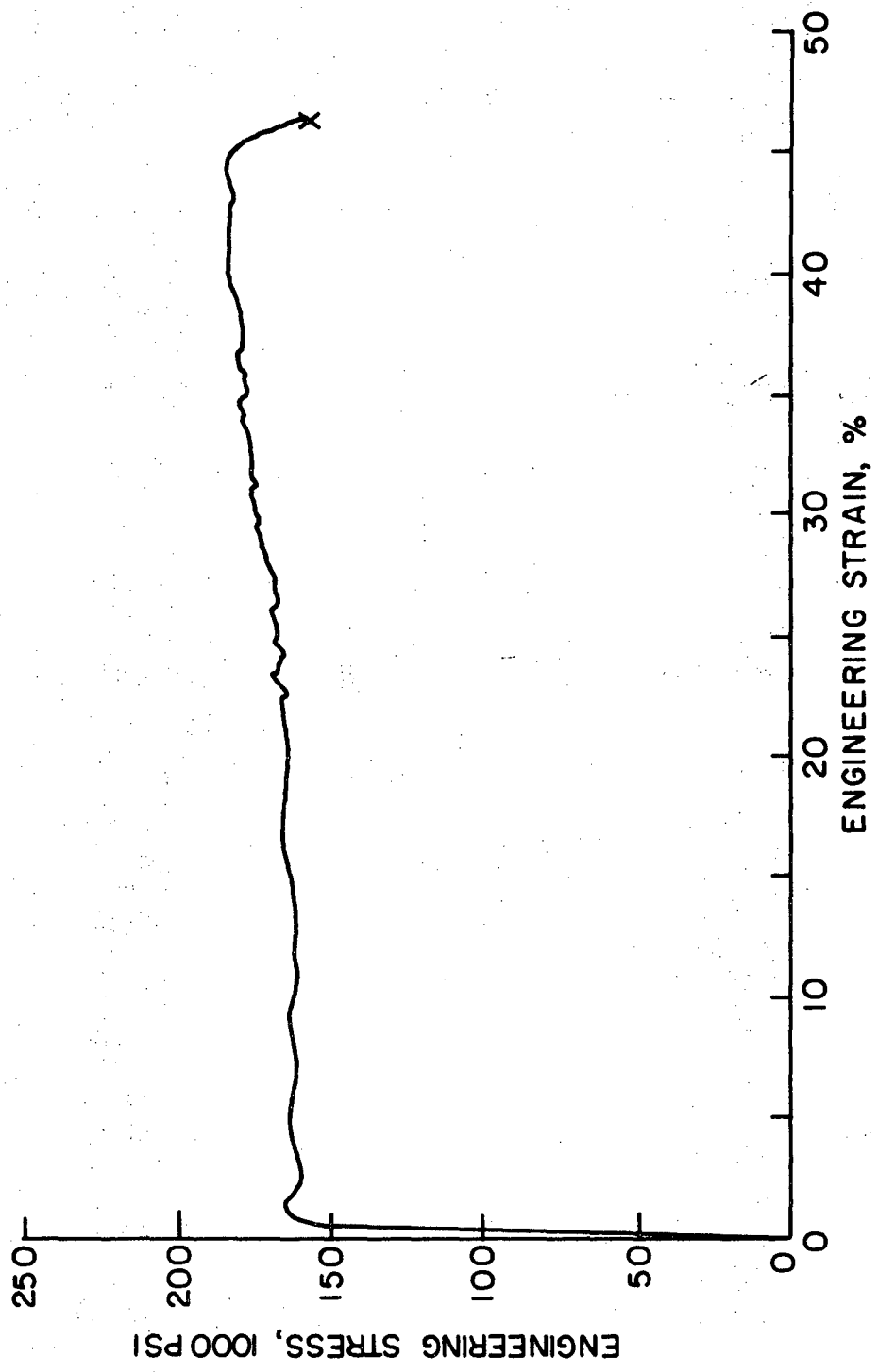
XBL 708-1884

Fig. 3
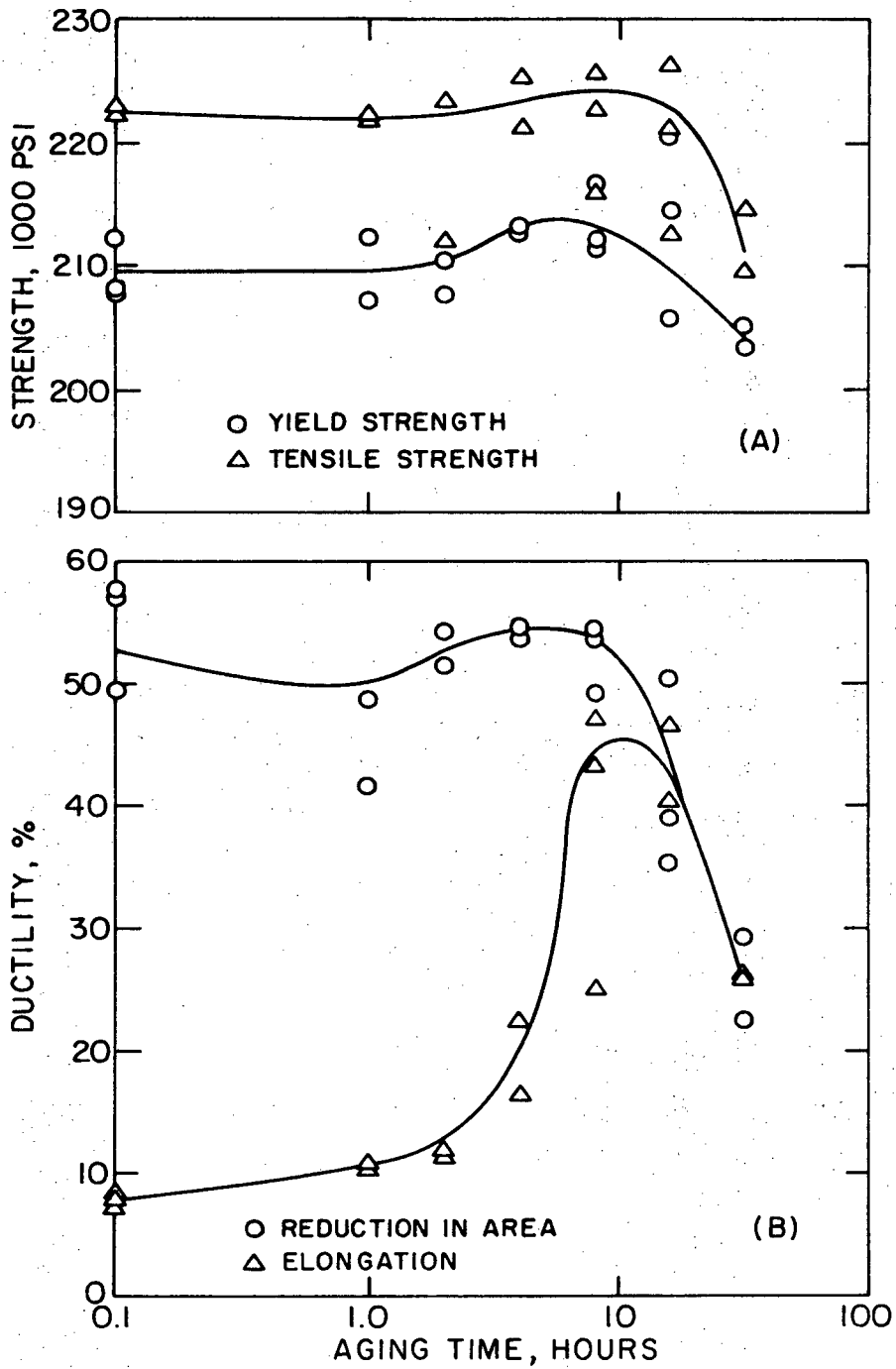
XBL 708-1875

Fig. 4
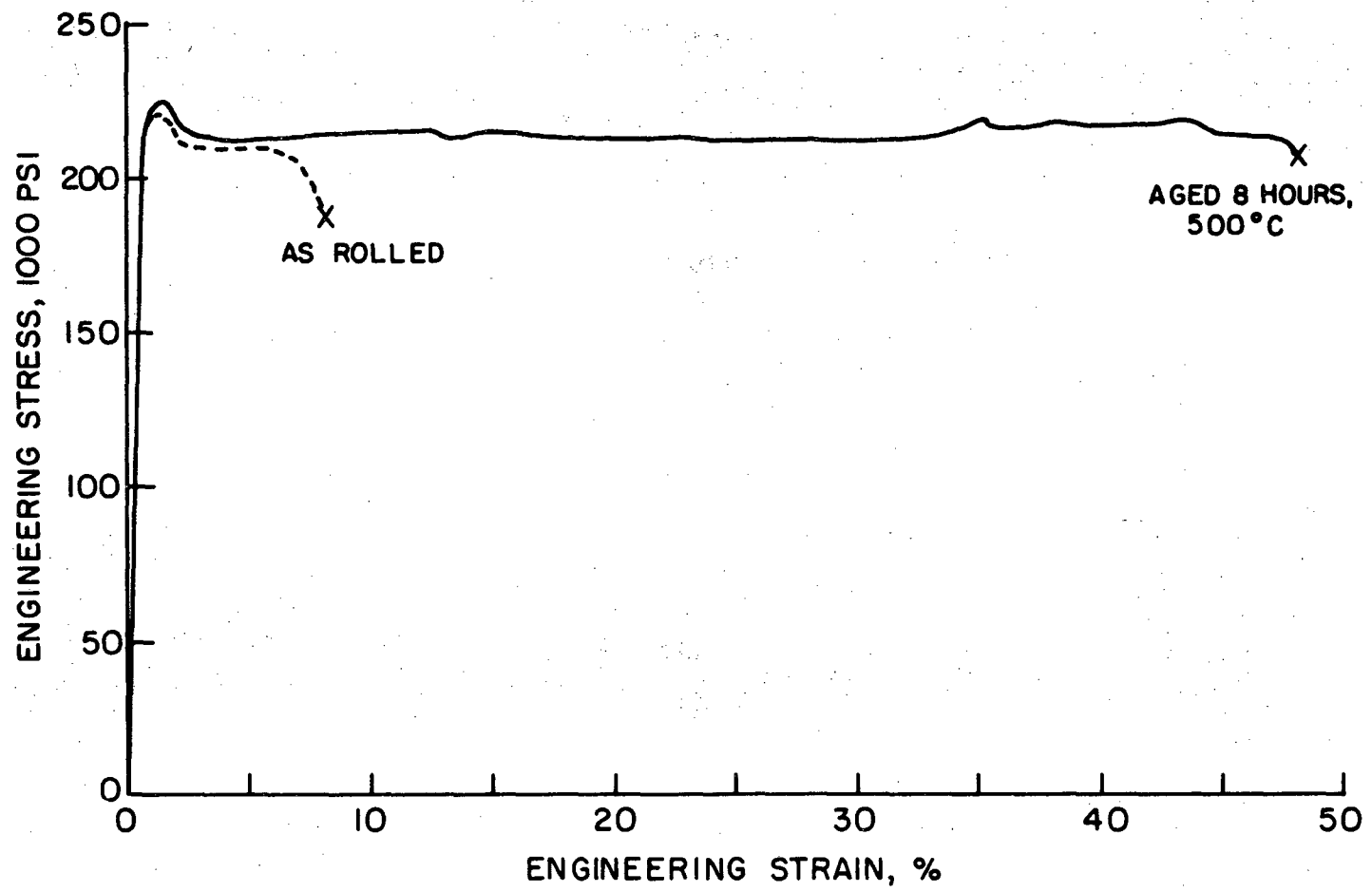
Fig. 5

XBL 708-1911

-45-
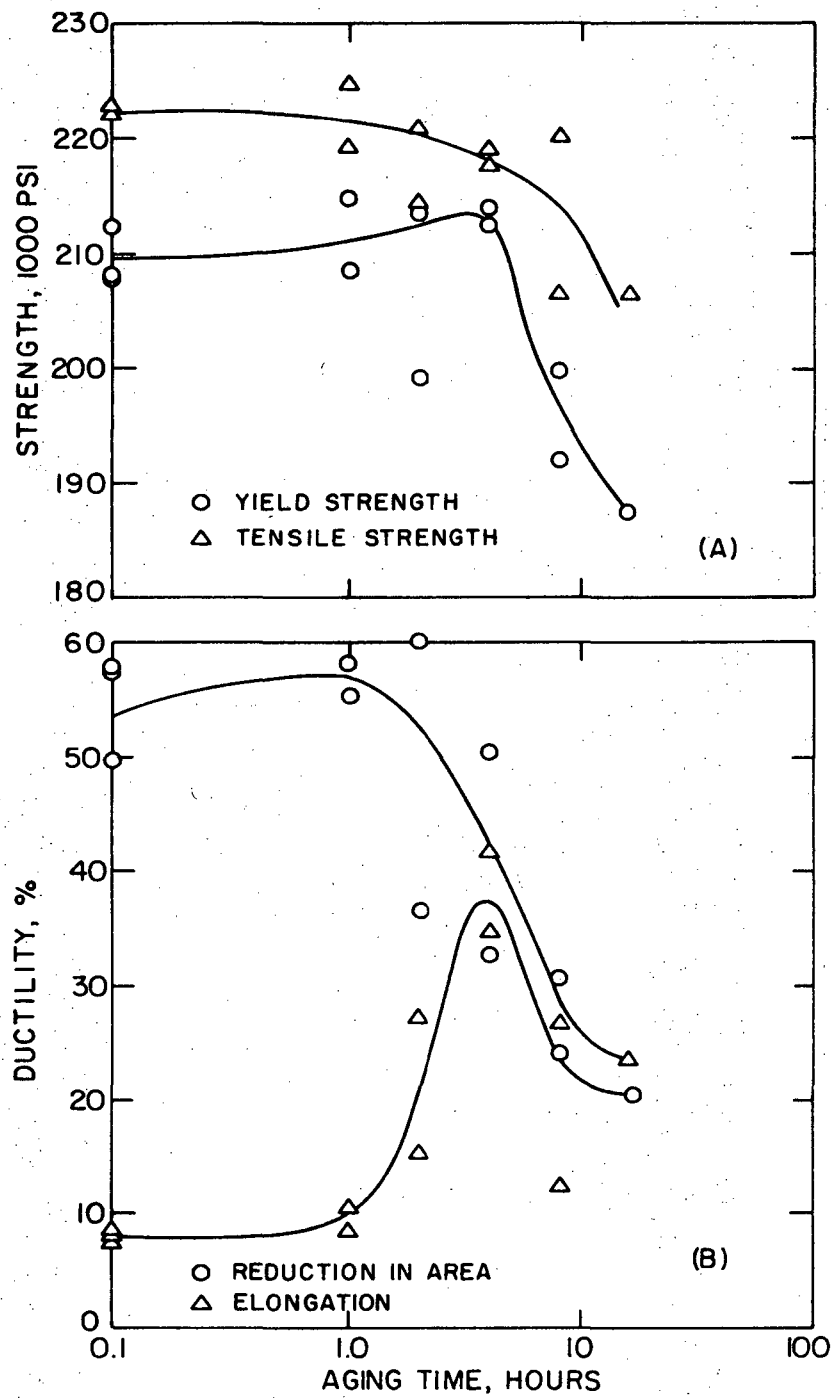
XBL 708-1877

Fig. 6

XBL 708-1878

Fig. 7

(A)

(B)
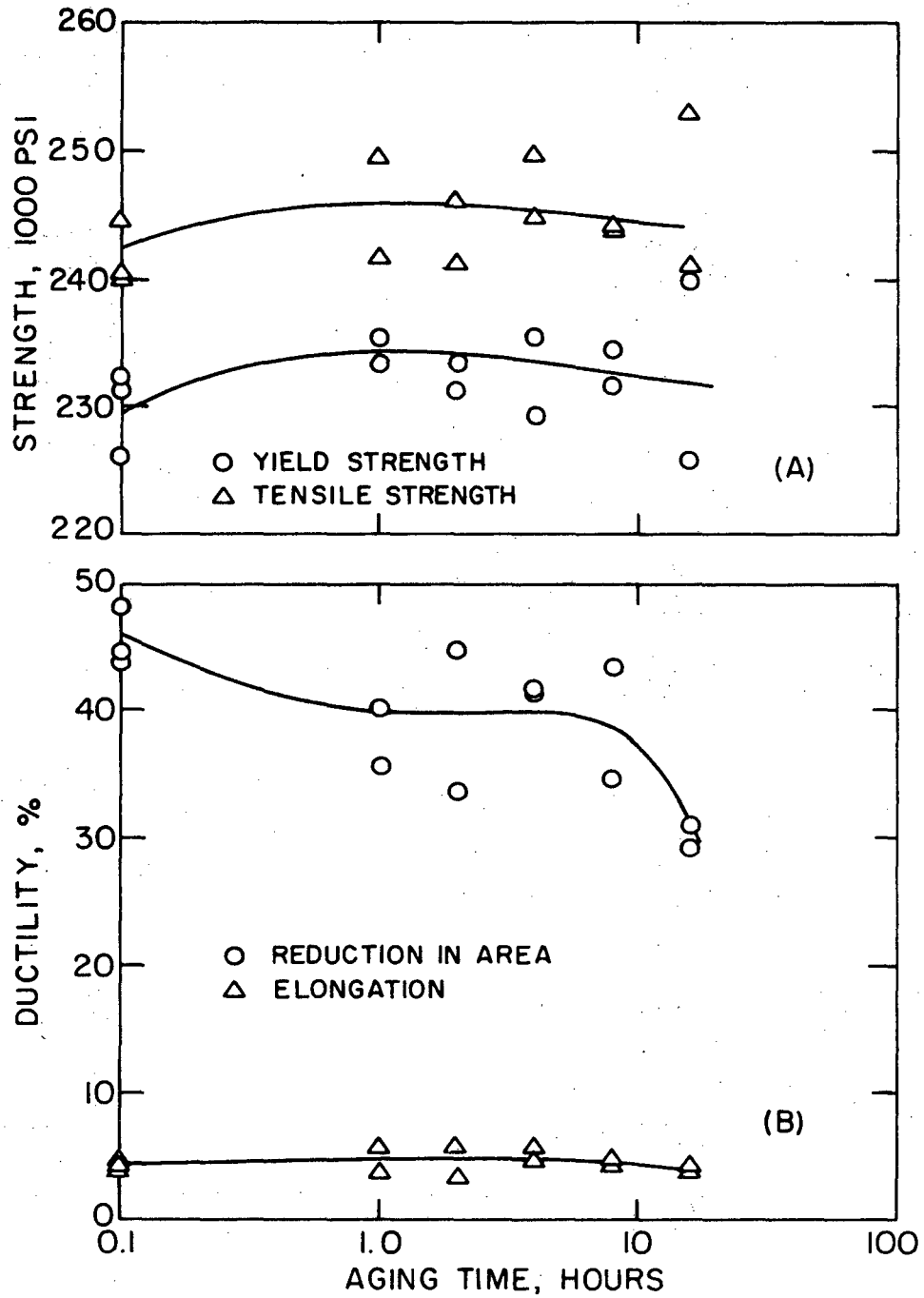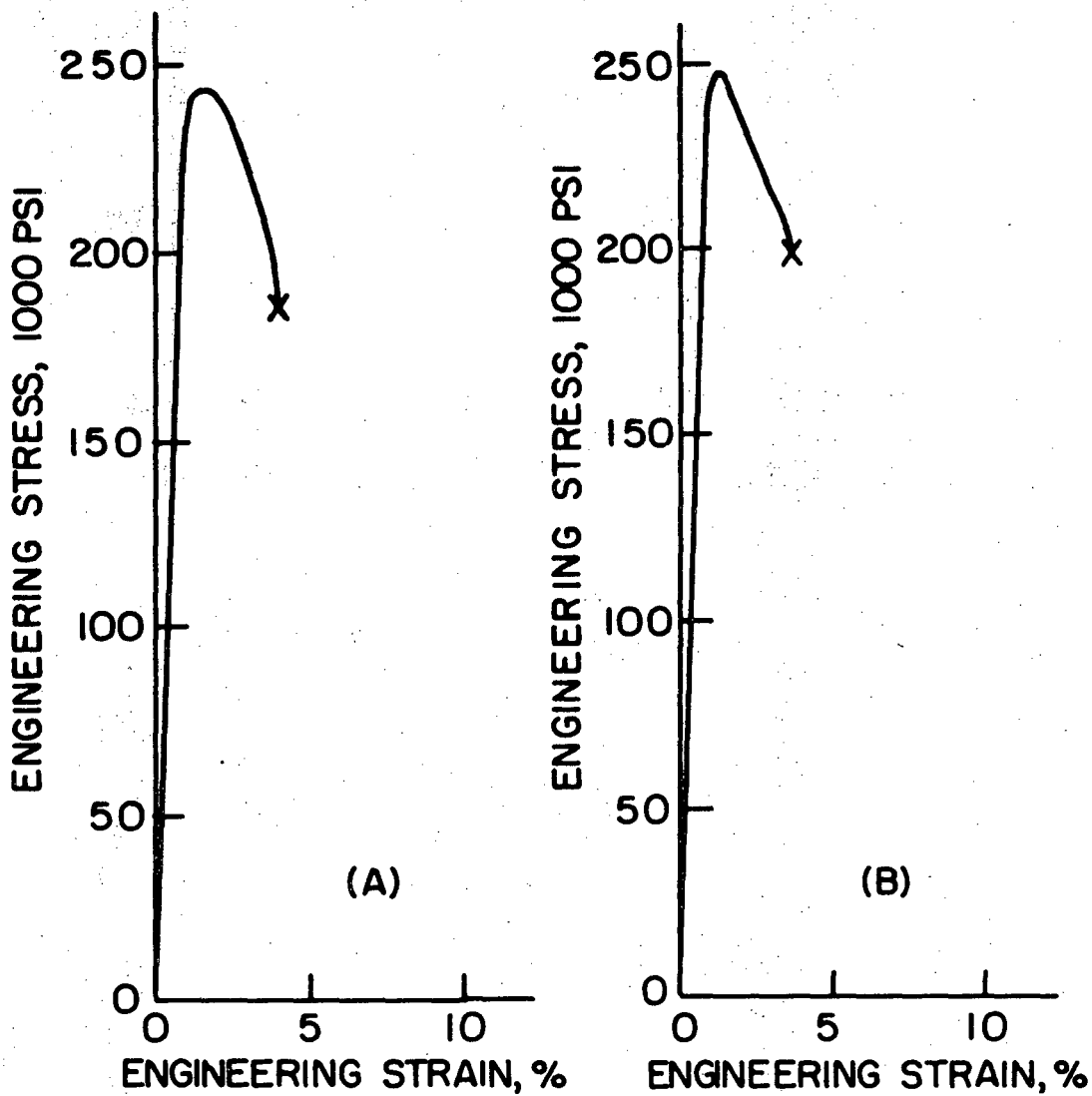
XBL 708-1883

Fig. 8
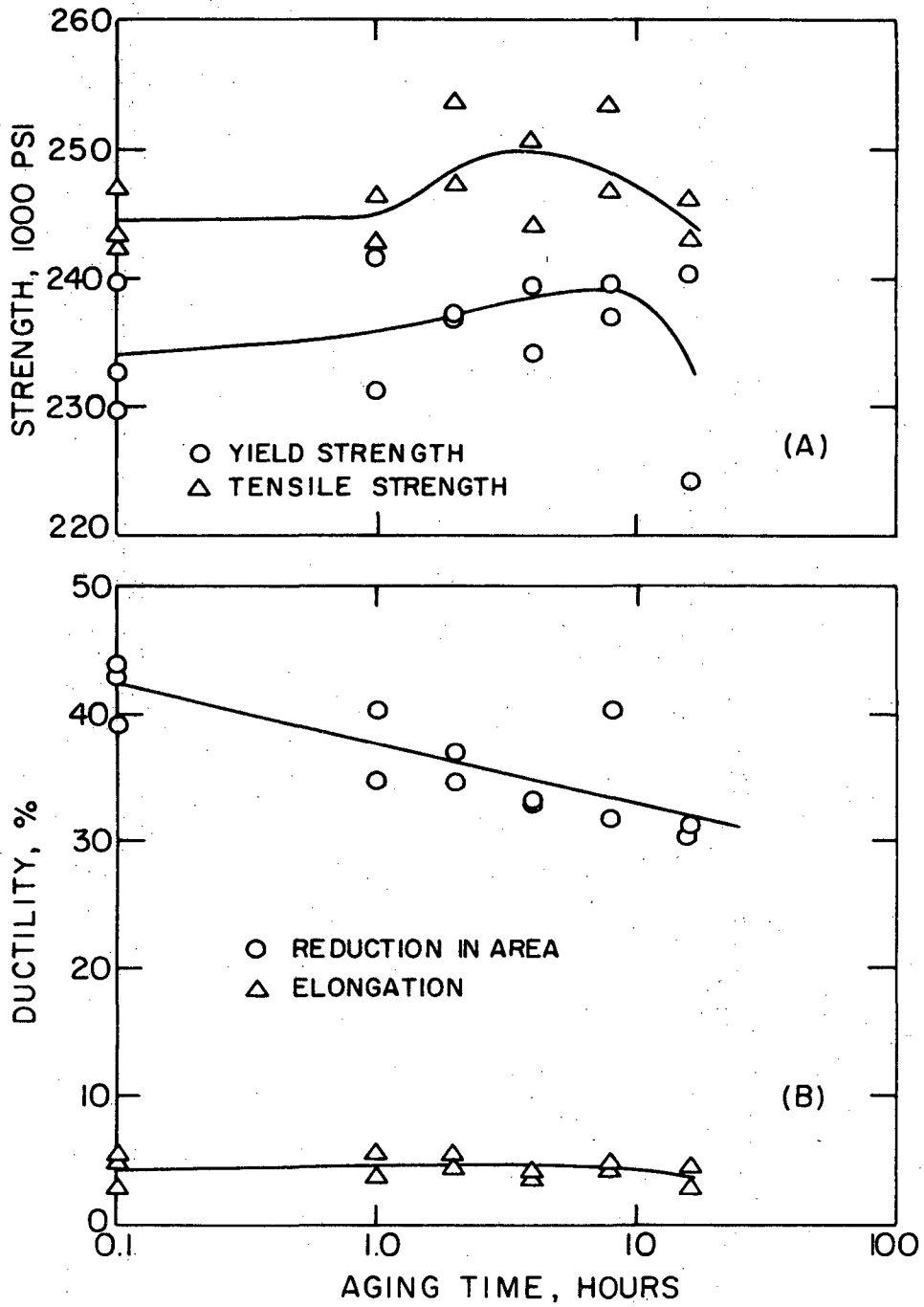
XBL 708-1880

Fig. 9
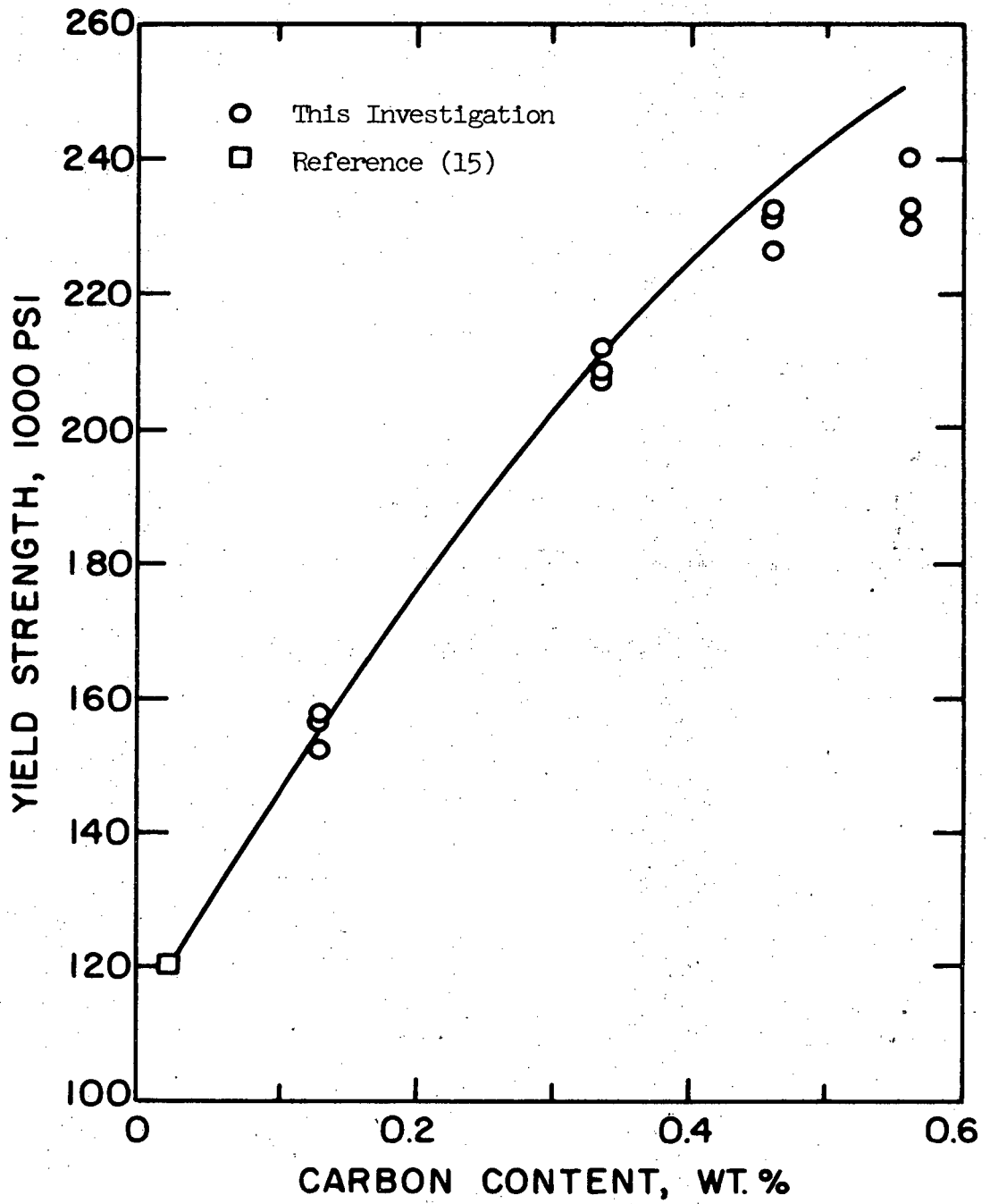
XBL 708-1879

Fig. 10
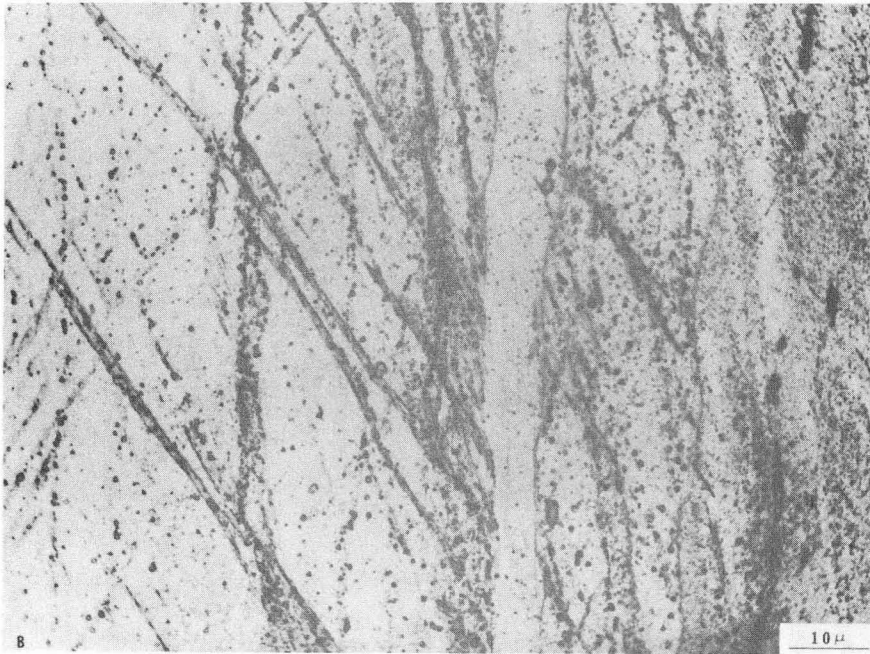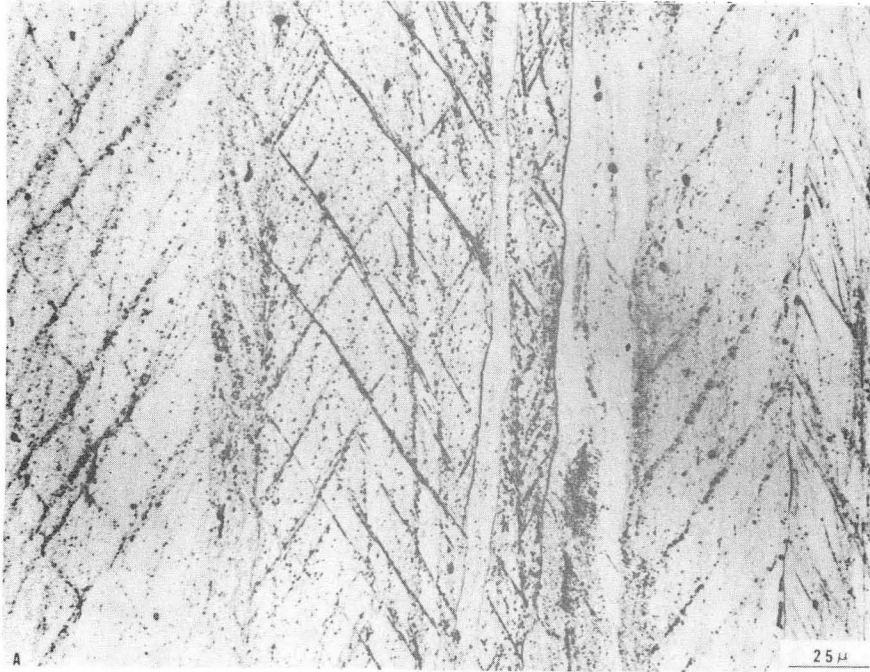
XBB 708-3681

Fig. 11
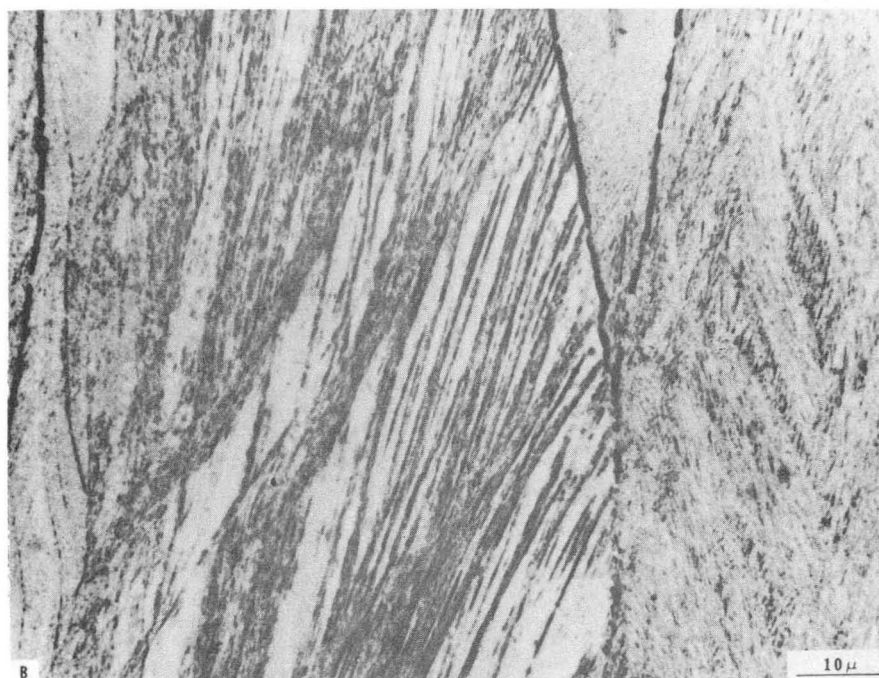
Fig. 12

XBB 708-3683

Fig. 13

100μ

XBB 708-3684

Fig. 14

25μ
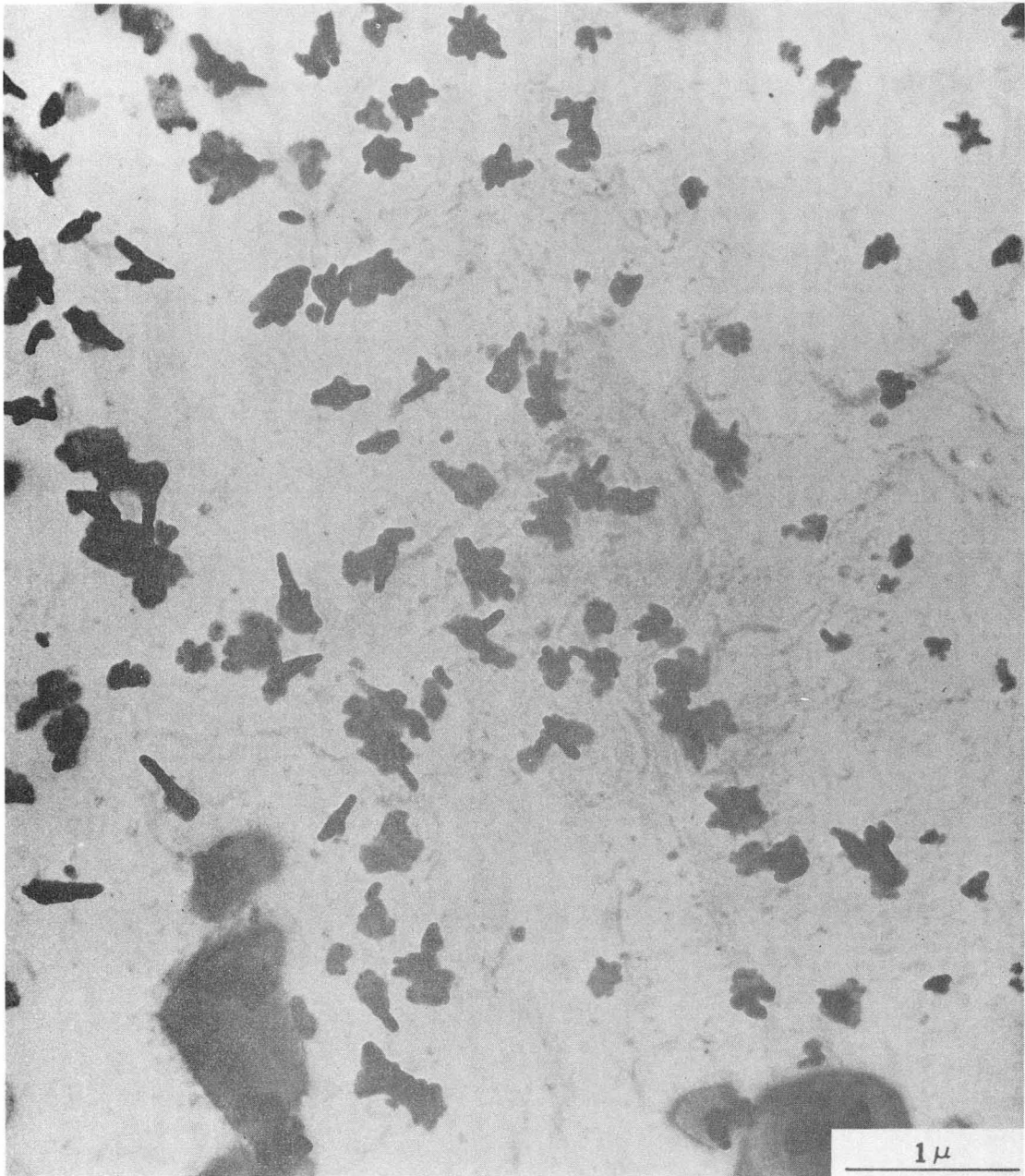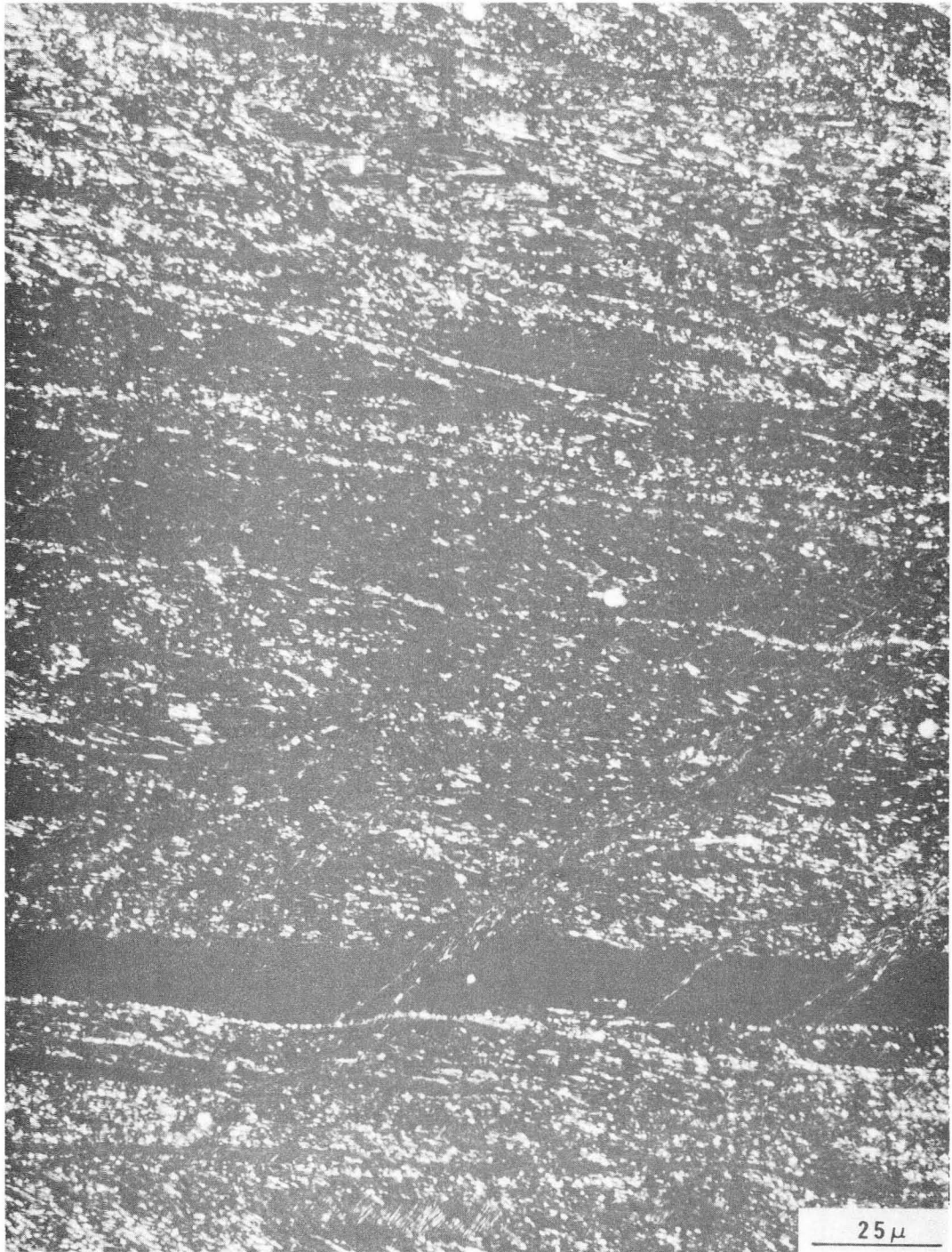
XBB 708-3682

Fig. 15
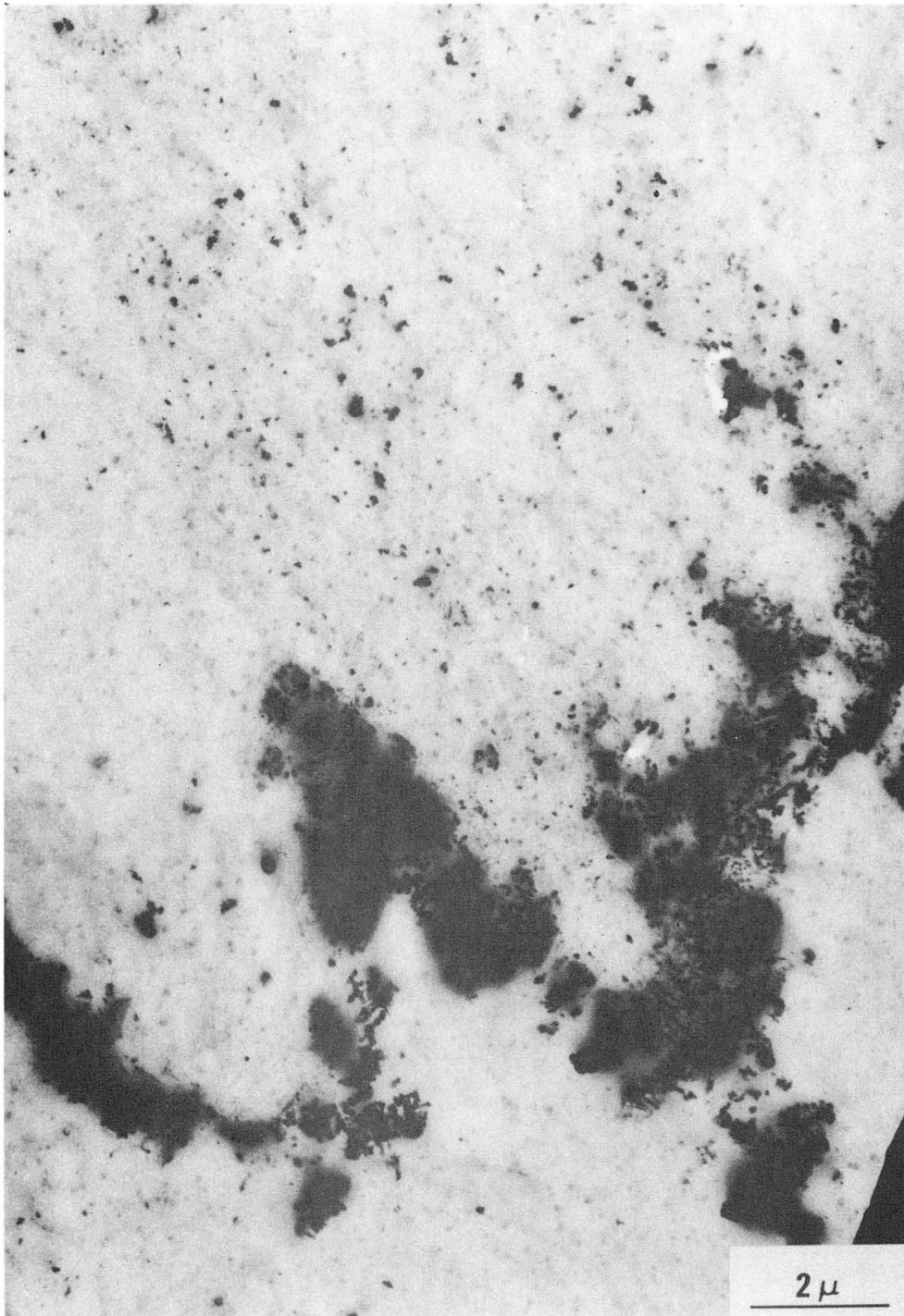
XBB 708-3679

Fig. 16
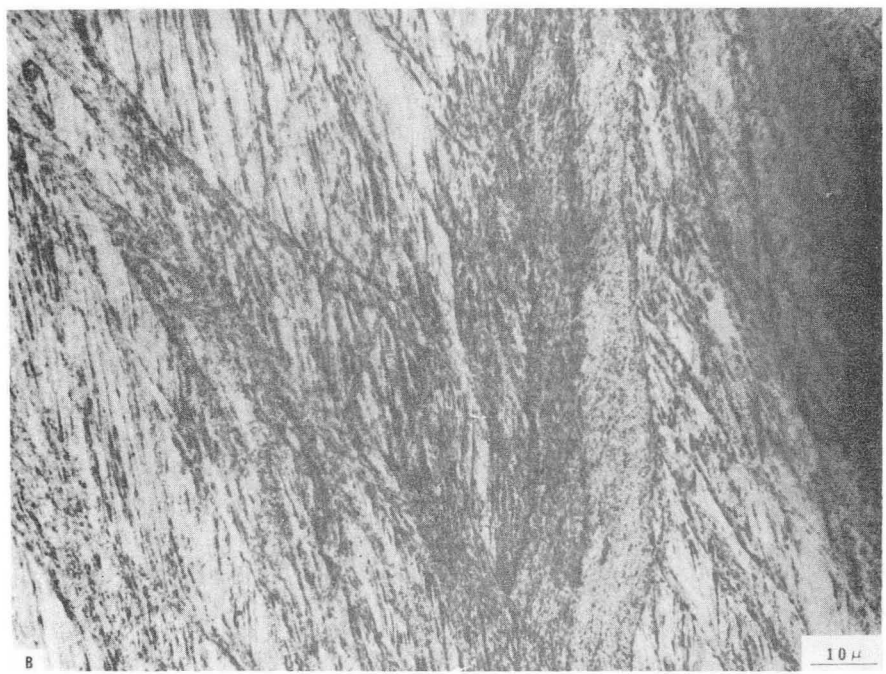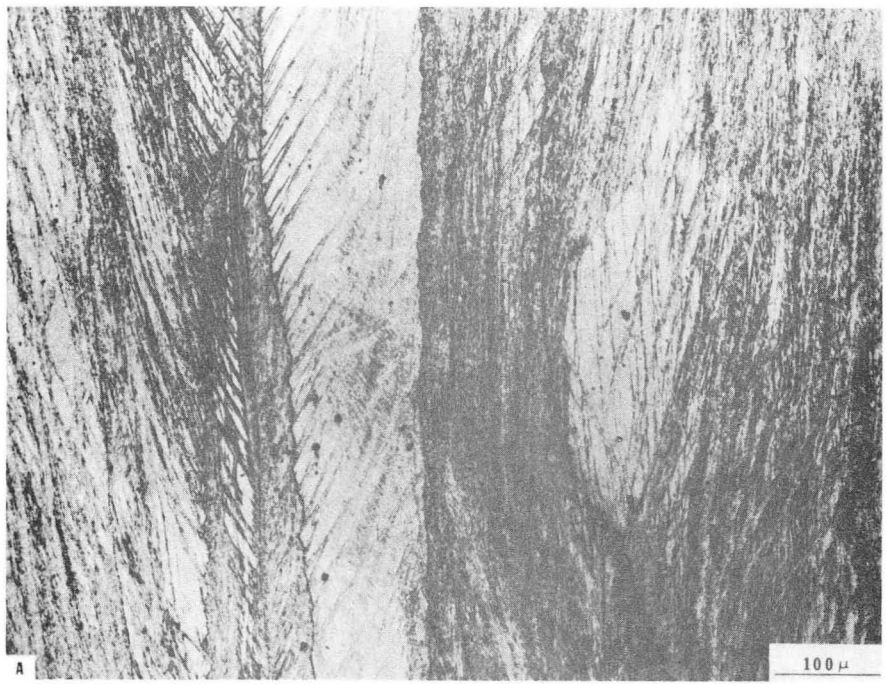
XBB 708-3686

Fig. 17
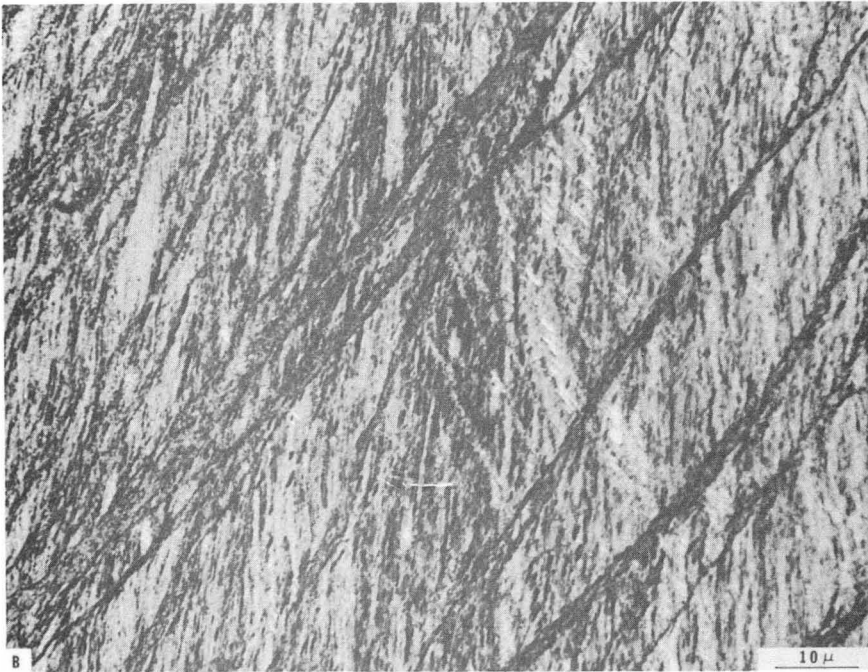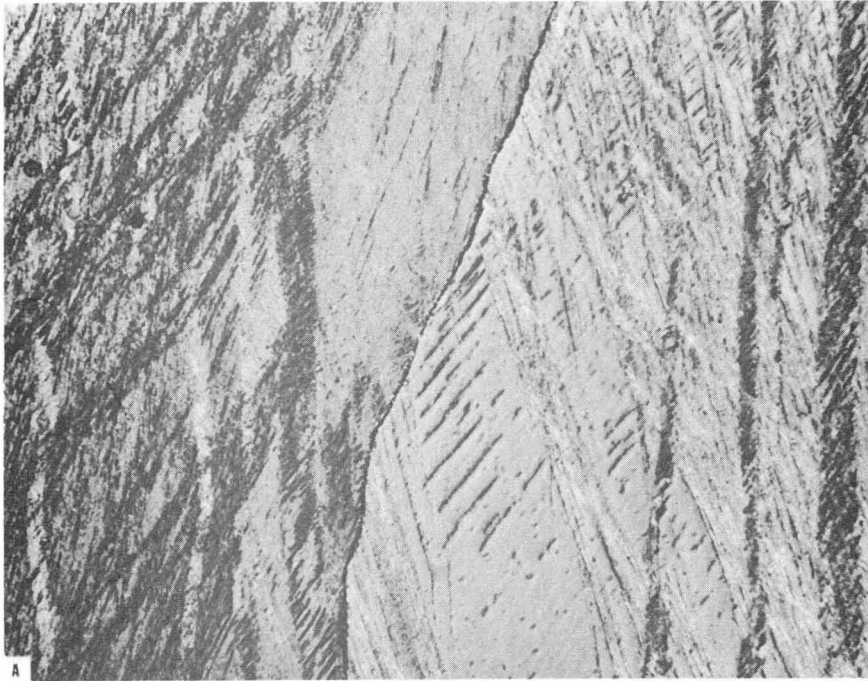
XBB 708-3680

Fig. 18
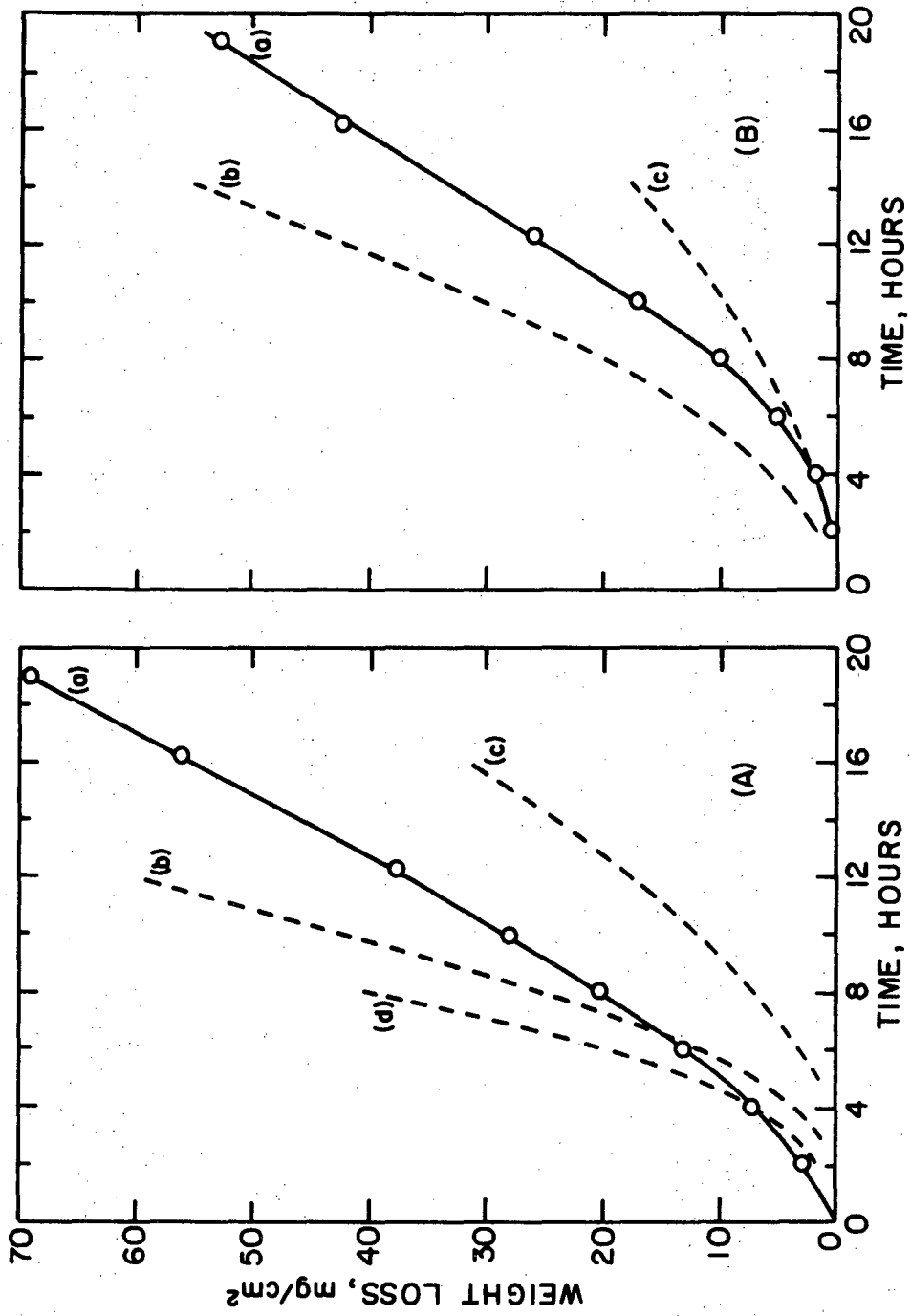
XBL 708-1881

Fig. 19

XBL 708-1876

Fig. 20

302   304   A-as rolled   B-as rolled

B-aged 8 hrs
at 500°C   C-as rolled   D-as rolled

XBB 708-3678

Fig. 21